https://doi.org/10.1093/plphys/kiac441 PLANT PHYSIOLOGY 2022: 190: 2775–2796

Plant Physiology®

Research Article

Ethylene response factor ERF.D7 activates *auxin response factor 2* paralogs to regulate tomato fruit ripening

Priya Gambhir [1], **Vijendra Singh** [1], **Adwaita Parida** [1], **Utkarsh Raghuvanshi** [1], **Rahul Kumar** [2,*] **and Arun Kumar Sharma** [1,*]

1 Department of Plant Molecular Biology, University of Delhi South Campus, New Delhi 110021, India
2 Department of Plant Sciences, School of Life Sciences, University of Hyderabad, Hyderabad 500046, India

*Author for correspondence: arun.sharma@south.du.ac.in (A.K.S.), rksl@uohyd.ac.in (R.K.)
These authors contributed equally (V.S. and A.P.)
A.K.S. and R.K.: conceptualization. P.G., A.P., U.R., R.K., and V.S.: investigation, validation, methodology, and formal analysis. P.G.: writing original draft. A.K.S. and R.K.: reviewing, editing, and supervision.
The author responsible for distribution of materials integral to the findings presented in this article in accordance with the policy described in the Instructions for Authors (https://academic.oup.com/plphys/pages/general-instructions) is: Arun K. Sharma (arun.sharma@south.du.ac.in).

Abstract

Despite the obligatory role of ethylene in climacteric fruit ripening and the identification of 77 ethylene response factors (ERFs) in the tomato (*Solanum lycopersicum*) genome, the role of few ERFs has been validated in the ripening process. Here, using a comprehensive morpho-physiological, molecular, and biochemical approach, we demonstrate the regulatory role of ERF D7 (SlERF.D7) in tomato fruit ripening. *SlERF.D7* expression positively responded to exogenous ethylene and auxin treatments, most likely in a ripening inhibitor-independent manner. *SlERF.D7* overexpression (OE) promoted ripening, and its silencing had the opposite effect. Alterations in its expression modulated ethylene production, pigment accumulation, and fruit firmness. Consistently, genes involved in ethylene biosynthesis and signaling, lycopene biosynthesis, and cell wall loosening were upregulated in the OE lines and downregulated in RNAi lines. These transgenic lines also accumulated altered levels of indole-3-acetic acid at late-breaker stages. A positive association between *auxin response factor 2* (*ARF2*) paralog's transcripts and *SlERF.D7* mRNA levels and that *SlARF2A* and *SlARF2B* are direct targets of SlERF.D7 underpinned the perturbed auxin–ethylene crosstalk for the altered ripening program observed in the transgenic fruits. Overall, this study uncovers that SlERF.D7 positively regulates SlARF2A/B abundance to amalgamate auxin and ethylene signaling pathways for controlling tomato fruit ripening.

Introduction

Owing to the agronomical position tomato (*Solanum lycopersicum*) upholds, a comprehensive dissection of its intrinsic ripening program is imperative to unravel the molecular mechanisms governing vital qualitative and quantitative fruit-related traits. The original concept of the fruit maturation process in climacteric fruits is based on a classic linear prototype guided by the precise spatio-temporal expression of the genes of ethylene biosynthesis and signaling (Alba et al., 2005; Kumar et al., 2016; Sravankumar et al., 2018). However, zooming in on the transcription networks activated during ripening in fleshy fruits has revealed a well-defined information system in which a multitude of hidden layers tightly control the ethylene biosynthesis and signaling

Received July 11, 2022. Accepted August 27, 2022. Advance access publication September 21, 2022

to produce ripened fruits as an output. One such regulatory circuit involves crosstalk between ethylene and auxin, in which the latter antagonistically targets major facets of ethylene-regulated fruit ripening (Böttcher et al., 2010; Schaffer et al., 2013; Sravankumar et al., 2018). Auxin and ethylene are two cornerstones of overall fruit development and are assumed to be involved in inevitable trade-offs, that is, the ability of ethylene to trigger fruit ripening occurs at the expense of disruption of auxin biosynthetic and signaling machinery (Given et al., 1988; Zaharah et al., 2012; Kumar et al., 2014; Sravankumar et al., 2018). Experimental validation of this trade-off was reported when the exogeneous application of auxin inhibitor, *p*-chlorophenoxyisobutyric acid, to tomato fruits mimicked 1-aminocyclopropane-1-carboxylic acid (ACC) treatment and displayed early signs of fruit ripening (Su et al., 2015).

Deepening insights into the connection between signal transduction components of auxin and ethylene roots back to the era of identification of ethylene insensitive mutants with defects in auxin transporters, *aux1* and *ethylene insensitive root1/pinformed 2* (*eir1/pin2*) (Pickett et al., 1990; Luschnig et al., 1998). These mutants exhibited root growth inhibition synergistic with the effect of auxin on this process (Rahman et al., 2001; Swarup et al., 2002). Apart from being collaborators, ethylene and auxin have exemplified competitiveness in lateral root initiation in thale cress (*Arabidopsis thaliana*) whereby auxin have been shown to promote lateral root formation, and elongation with ethylene negatively regulated the primary as well as lateral root elongation (Ivanchenko et al., 2008; Negi et al., 2008, 2010; Muday et al., 2012). The centrality of auxins in defining regions of meristem growth in roots and shoots has long been recognized (Benková et al., 2003; Blilou et al., 2005). What is fascinating is that the pattern of auxin transport in these regions is strongly influenced by ethylene (Růžička et al., 2007). Once accumulated, auxin then initiates the repression of ethylene mediated root growth phenotype (Lewis et al., 2011). Additionally, the points of convergence between auxin and ethylene at the transcriptional level have been extensively studied due to documentation of their receptor and signaling mutants in the public domain. Ethylene-insensitive root growth phenotypes were observed in auxin receptor mutant *Transport inhibitor response 1* (*TIR1*), auxin transport mutants (*AUX1* and *EIR/AGR/PIN2*) as well as in mutants deficient in auxin response (*AXR2/IAA7* and *AXR3/IAA17*) (Pickett et al., 1990; Luschnig et al., 1998; Stepanova et al., 2005; Muday et al., 2012). In parallel, ethylene receptors are up-regulated in fruits by auxins (Gillaspy et al., 1993; Jones et al., 2002; Trainotti et al., 2007). These points of intersection serve two separate and important roles: regulating global plant architecture and conferring local robustness on development.

In climacteric fruits, an absolute requirement of increased ethylene production via the upregulation of *1-aminocyclopropane-1-carboxylate synthase 2* (*ACS2*) and *1-aminocyclopropane-1-carboxylate oxidase 1* (*ACO1*) transcripts coordinated with low auxin levels sets the stage for ripening (Alba et al., 2005; Sravankumar et al., 2018). Interestingly, mRNA levels of *ACS2*, *ACS4*, and *ACO1* are upregulated by auxin in tomato and peach (Jones et al., 2002; Trainotti et al., 2007). The physiological effects of both the hormones, at the genetic level, are brought about by their main transcriptional regulators, such as EIN3-like proteins (EILs) and ethylene response factors (ERFs) in the case of ethylene and auxin response factors (ARFs), AUX/indole-3-acetic acid (IAA), and Topless proteins in the case of auxin. Genome-wide identification studies have revealed that the tomato genome harbors 77 ERF (Sharma et al., 2010; Pirrello et al., 2012) and 22 ARF members. Accumulated evidence shows that ethylene controls the accumulation of some ARF transcripts during tomato fruit development signifying the possibility of involvement of auxin in climacteric fruit ripening (Jones et al., 2002). Likewise, several ERF genes are regulated by auxin (Trainotti et al., 2007; Pirrello et al., 2012). This two-way communication channel is feasible due to the multi-member gene families of ERFs and ARFs and the presence of both auxin and ethylene cis-regulatory elements in the promoter regions of these two sets of transcription factors (Muday et al., 2012; Zouine et al., 2014). Consistent with antagonism to ethylene, tomato fruit firmness and sugar metabolism have been reported to be partly regulated by *SlARF4* (Jones et al., 2002; Sagar et al., 2013). More recently, another ARF, *SlARF2* has been proven to be a quintessential component of the regulatory network controlling fruit ripening. Silencing of *SlARF2* brought about dramatic ripening defects with a concomitant reduction in ethylene production and down-regulation of key ripening regulators *RIN*, *NOR*, and *CNR* in tomato (Hao et al., 2015; Breitel et al., 2016).

Several ripening-induced ERF genes have been implicated in the regulation of fruit ripening in tomato (Sharma et al., 2010; Liu et al., 2014, 2016). Overexpression (OE) of one such gene, *LeERF1*, resulted in constitutive ethylene response with accelerated fruit ripening and enhanced fruit softening (Li et al., 2007; Liu et al., 2015). Another key piece of evidence further substantiating the importance of ERFs in ripening has come from *SlERF6*, which integrates ethylene and carotenoid pathways in tomato (Lee et al., 2012; Liu et al., 2016). Due to the issue of proposed overlapping functions among ERF members, evidence for the involvement of another ERF, *SlERF.B3*, in controlling carotenoid accumulation and ethylene production was demonstrated using a dominant repressor strategy (Liu et al., 2014). Although the contribution of a few of the ripening-induced ERFs in tomato fruit ripening has been elucidated, the function of the majority of these genes largely remains undocumented. Moreover, due to the constitutive OE or silencing of these genes in earlier studies, pleiotropic phenotypes unrelated to fruit ripening have also been reported (Li et al., 2007; Liu et al., 2018). Previously, we have identified and reported several ripening-induced ERFs (Sharma et al., 2010; Kumar et al., 2012a; Srivastava and Kumar, 2019). We have also

characterized a fruit ripening-specific *RIP1* promoter (Agarwal et al., 2017). In the present study, we report the functional validation of a yet to be described ripening-induced ERF gene, *SlERF.D7*, for its roles in the regulation of fruit ripening traits in tomato by silencing it under *RIP1* promoter. First, we report that *SlERF.D7* transcripts are inhibited during fruit ripening in *rin* and *nor* mutants and *in-house* RIN-silenced lines (Kumar et al., 2012a). Transcript profiling using reverse transcription-quantitative PCR (RT-qPCR) revealed strong induction of *SlERF.D7* mRNA levels upon exogenous ethylene and auxin applications. Using a reverse genetic approach, we demonstrate that *SlERF.D7* plays a pivotal role in fruit ripening via directly modulating the expression of *SlARF2*, thereby serving as a critical point of intersection between ethylene and auxin signaling pathways. Fruit-specific silencing of *SlERF.D7* under *RIP1* promoter results in a severe reduction in ethylene production, fruit firmness, and pigment accumulation of the transgenic fruit, a phenotype that resembles the *SlARF2* down-regulation line fruits (Hao et al., 2015; Breitel et al., 2016). In contrast, *RIP1* driven ripening-specific OE of *SlERF.D7* fastened the ripening progression and enhanced fruit lycopene levels. Thus, using a suite of morpho-physiological, biochemical, pharmacological, and molecular tools, we identify a regulator of tomato fruit ripening and provide critical insight into the auxin–ethylene controlled molecular circuitry that controls the ripening traits in tomato.

Results

Transcript profiling of *SlERF.D7* reveals a potential role in fruit ripening

First, to predict the function of SlERF.D7, its transcript abundance was assessed by RT-qPCR in different plant tissues/organs/stages, including cotyledons, leaf, stem, root, flower, and at different stages of tomato fruit development and ripening. The transcript levels of *SlERF.D7* were found to be low in vegetative organs. In contrast, it displayed a drastic up-regulation at the 5 days post breaker (Br) stage and reached its maximum levels at 10 days post Br, indicating its prospective requirement in the ripening process (Figure 1A). Next, we evaluated its mRNA abundance at different ripening stages, namely mature green (MG), Br, 3 days post Br (Br + 3), 5 days post Br (Br + 5), and 10 days post Br (Br + 10) in wild-type (WT), RIAI05, and RIAI06 transgenic lines and same-age fruits of two ripening mutants, *ripening-inhibitor* (*rin*) and *non-ripening* (*nor*) (Figure 1, B and C). Contrary to the WT fruits, the RT-qPCR analysis revealed no ripening-associated induction of *SlERF.D7* transcripts at B + 5 and B + 10 stages in *rin* mutant fruits (Figure 1B). However, fruits from RIN suppressed transgenic lines (RIA105 and RIAI06), and *nor* mutant fruits exhibited a slight increase in the expression level of *SlERF.D7* at late-Br stages, but the enhancement was significantly lower than the WT fruits. These results indicated the functional relevance of the *SlERF.D7* gene during tomato fruit ripening.

SlERF.D7 is a nuclear-localized gene that responds positively to exogenous auxin and ethylene treatment

Next, we studied the subcellular localization of SlERF.D7 by transiently expressing *SlERF.D7::GFP* construct in *Nicotiana benthamiana* leaves. The *CaMV35S*-driven *SlERF.D7::GFP* fusion protein was found to be exclusively localized to the nucleus, consistent with its putative role in transcriptional regulation (Figure 1D and Supplemental Figure S1). To further characterize the SlERF.D7 protein, we determined its transactivation potential via transient expression assay using a GAL4-responsive reporter system. As hypothesized, SlERF.D7 displayed a strong transcriptional activation potential in the yeast system (Figure 2A).

We have previously observed the activation of ethylene-related ripening-associated genes by exogenous auxin treatment and vice versa (Kumar et al., 2012a; Sravankumar et al., 2018). Mining of the 2.5-kb upstream sequence of *SlERF.D7* for cis-acting regulatory elements using the PLACE/signal search tool (http://www.dna.affrc.go.jp/PLACE/signalscan.html) revealed the presence of two putative ethylene response elements (ERE-CCGAC) and two auxin response elements (AuxRE-TGTCTC) in its promoter region (Figure 2B). Furthermore, a putative fruit-specific element variant with a sequence motif TCTTCACA was also identified in the promoter region. We next investigated the influence of these two hormones on the transcriptional regulation of *SlERF.D7*. Exogenous treatment of both ethylene and auxin led to induction of *SlERF.D7* mRNA levels (Figure 2C). Furthermore, a decline in its mRNA levels upon treatment with either 1-methylcyclopropane (1-MCP) (100 μM), an inhibitor of ethylene perception, or *p*-chlorophenoxyisobutyric acid (PCIB) (100 μM), an antagonist of auxin function, validated the positive effect of both ethylene and auxin on *SlERF.D7* transcription (Figure 2C). We estimated the efficacy of hormonal treatments by evaluating the transcript abundance of known ethylene (*E8*) and auxin (*SAUR*) responsive genes.

SlERF.D7 is not transcriptionally activated by RIN

MADS-box proteins such as RIN, TAGL1, FUL1, and FUL2 have been previously reported to bind to CArG box elements in the promoters of ripening-related genes such as *SlACS2* and *SlPSY1* (Fujisawa et al., 2011; Li et al., 2019). The presence of a CArG box element in the upstream region of *SlERF.D7* (Figure 2B) instigated us to examine its direct regulation by the ripening master regulator RIN using yeast one-hybrid (Y1H) assay. Failure of survival of yeast cells containing both RIN protein and *SlERF.D7* promoter on selection media suggested no direct binding of RIN to the promoter. In contrast, yeast cells with RIN-activated *SlACS2* promoter, the positive control taken in the study, survived on the selection media, thereby conferring resistance in the cells to successfully grow on the selection medium (Figure 2D). To further corroborate this result in vivo, we conducted a transient transactivation assay of *SlERF.D7* promoter by RIN in *N. benthamiana* leaves using GUS and GFP reporter systems. For this purpose, 4-week-old *Nicotiana* leaves were

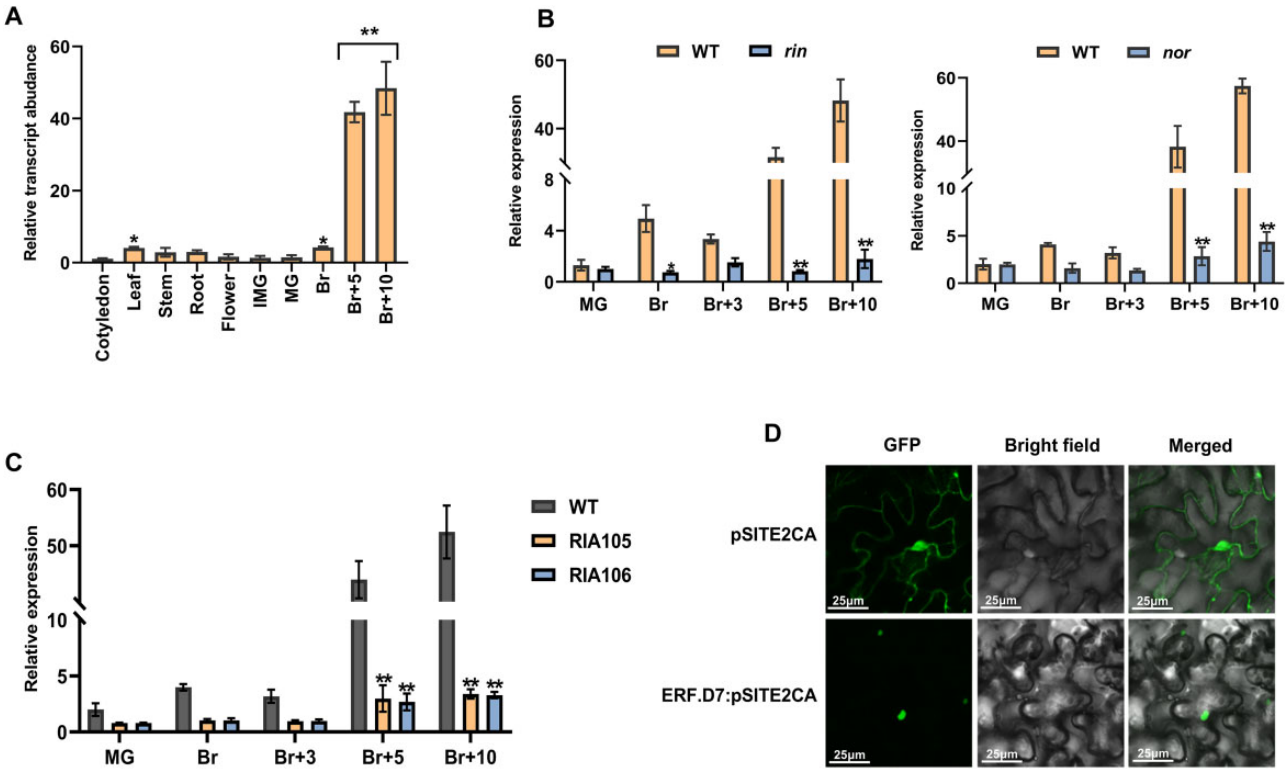

Figure 1 Transcript profiling of *SlERF.D7* (Solyc03g118190) and its subcellular localization. A, Expression of *SlERF.D7* in various tissues, including cotyledon, roots, stems, leaves, flowers, and fruit at different developmental stages: immature green (IMG), MG, Br, 5-day after Br (Br + 5), and 10-day after Br (Br + 10) in WT (Pusa Ruby). Values are means ± SD of three independent replicates. Asterisks indicate the statistical significance using ANOVA: *, 0.01 < *P*-value < 0.05; **, 0.001 < *P*-value < 0.01. B and C, Relative expression levels (in fold change) of *SlERF.D7* in WT (Ailsa Craig), *ripening-inhibitor* (*rin*; accession no. LA1795, in the unknown background) mutant and *nor* mutant (in Ailsa Craig background), and 3S:RIN knockdown lines (RIA105 and RIA106; in Pusa Ruby background) at various stages of fruit ripening. Expression profiles were studied at different stages of fruit ripening by employing the RT-qPCR technique. The mRNA levels of *SlERF.D7* at the MG stage in WT were used as the reference for all stages. Values are means ± SD of three independent replicates. Asterisks indicate the statistical significance using Student's *t* test: *, 0.01 < *P*-value < 0.05; **, 0.001 < *P*-value < 0.01. D, Subcellular localization of SlERF-D7 in the nucleus of *N. benthamiana* epidermal cells.

co-infiltrated with the effector construct carrying the *RIN* coding sequence (CDS) driven by the *CAMV35S* promoter. The reporter constructs were GUS or GFP CDSs driven by *SlERF.D7* promoter. As noticed in the Y1H assay, there was no significant alteration in *SlERF.D7*-driven GUS activity or GFP fluorescence, in contrast to the positive control *SlACS2* driven enhanced GUS activity and GFP fluorescence transactivation assays confirming that RIN is incapable of binding to the *SlERF.D7* promoter (Figure 2E). These observations indicated that *SlERF.D7* induction during fruit ripening is independent of RIN.

Ripening-specific over-expression and silencing of *SlERF.D7* display dramatic but contrasting ripening-related changes in the transgenic fruits

To further elucidate the role of SlERF.D7 in tomato fruit ripening, we generated *SlERF.D7* over-expression and RNAi knock-down transgenic lines in tomato cultivar "Pusa Ruby" under a ripening-specific *RIP1* promoter, characterized in our laboratory earlier (Figure 3A; Agarwal et al., 2017). *RIP1* gene is activated at post Br stage of ripening. A total of 12 independent over-expression and eight independent silencing transgenic lines were obtained (Supplemental Table S2 and Supplemental Figure S2). Based on fruits exhibiting the highest and the lowest transcript levels of *SlERF.D7*, we selected two homozygous T_2 generation representative transgenic lines for OE and silencing (RNAi) for further characterization. At the molecular level, the selected two OE lines, *SlERF.D7-OE#3* and *SlERF.D7-OE#11* exhibited the significantly elevated transcript accumulation at Br + 3 and Br + 10 stages compared with the tissue culture grown WT control fruits (Figure 3D). Similarly, two RNAi lines, *SlERF.D7-RNAi#1* and *SlERF.D7-RNAi#4*, displayed the strongest suppression of its transcripts, showing only 15%–20% accumulation of its WT fruits transcripts at the Br + 10 stage (Figure 3B). No visible phenotypic differences in plant height, flower phenotype, fruit morphology, fruit set, and fruit development in both OE and RNAi lines compared with the WT control plants were observed by us. Considering the ripening-related expression pattern of *SlERF.D7*, we next examined the phenotype of OE and RNAi transgenic fruits in detail. *SlERF.D7-OE#3* and *SlERF.D7-OE#11*

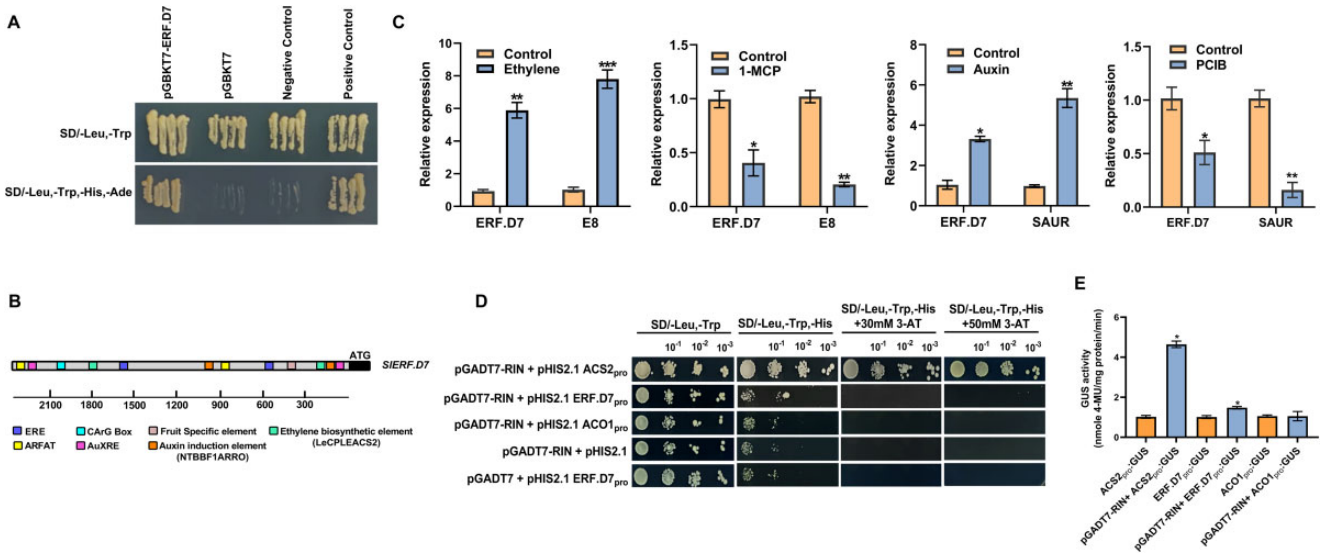

Figure 2 RIN-independent and ethylene- and auxin-dependent mode of action of SlERF.D7. A, Analysis of transactivation potential of SlERF.D7 in yeast by growing transformants on synthetic dextrose (SD) media-lacking leucine (Leu), tryptophan (Trp), histidine (His), and adenine (Ade). B, The presence of CArG Box, a putative fruit-specific element in addition to putative ethylene and AuxREs in the promoter of *SlERF.D7* gene. The cis-acting regulatory elements identified are represented by different color boxes. C, RT-qPCR analysis of *SlERF.D7* transcripts in total RNA samples extracted from WT MG fruit samples treated with 100 μM ethrel, 100 μM 1-MCP, 100 μM IAA, and 100 μM PCIB. Error bars, mean ± SD of three biological replicates. Asterisks indicate the statistical significance using Student's *t* test: *, 0.01 < *P*-value < 0.05; **, 0.001 < *P*-value < 0.01, *** *P*-value < 0.001. E8, an ethylene response gene; SAUR68, an auxin response gene. D and E, Identification of DNA binding activity of RIN to the promoter of *SlERF.D7* with (D) growth performance of transformants on SD/−Leu−/Trp/−His medium containing 50 mM 3-AT. Binding of RIN to the promoter of tomato *ACC synthase2* (*ACS2*) gene-: positive control, binding of RIN to the promoter of tomato *ACC oxidase1* (*ACO1*) gene-: negative control (E, in vivo interaction study of RIN to promoters of *SlERF.D7*, *SlACS2*, and *SlACO1* via GUS reporter assays in *N. benthamiana* leaves.

OE genotypes developed an intense red color at the Br + 10 stage compared with the WT fruits, whereas *SlERF.D7-RNAi#1* and *SlERF.D7-RNAi#4* fruits exhibited inhibited red color development and failed to turn fully red. The RNAi fruits developed a mottled ripening pattern with partial degradation of chlorophyll at the final ripe stage (Figure 3C). However, we noticed discernable phenotypic alterations pertaining to fruit softening in the fruits of *SlERF.D7 OE* lines as both *SlERF.D7-OE#3* and *SlERF.D7-OE#11* fruits displayed wrinkling of the outer pericarp tissue, possibly accounting for early signs of cell wall loosening than their WT controls (Figure 3C). Off-wine analysis of *SlERF.D7* OE and RNAi fruits exhibited the same ripening pattern, with OE lines fruits displaying signs of premature ripening compared with the WT control fruits. Contrastingly, *SlERF.D7* RNAi-silenced fruits showed less pigment accumulation coupled with increased firmness than their same-age WT control fruits (Figure 3D). Altogether, we observed contrasting fruit phenotypes regarding fruit color and chlorophyll degradation in OE and RNAi lines. These observations further indicated that the degradation of chlorophyll, synchronous with the synthesis of carotenoids and cell wall degradation during the ripening process, is directly targeted by *SlERF.D7*.

Down-regulation of *SlERF.D7* leads to reduced pigment accumulation and enhanced fruit firmness

To investigate the possible cause of altered pigmentation in *SlERF.D7* OE and RNAi fruits, we performed HPLC-based carotenoid profiling in WT and transgenic line pericarp tissue at MG, Br + 3, Br + 7, and Br + 10 stages. In terms of lycopene accumulation, a 55%–60% reduction was observed in SlERF.D7-RNAi#1 and SlERF.D7-RNAi#4 fruits compared with WT fruits at the Br + 10 stage. In contrast, the fruits of *SlERF.D7-OE#3* and *SlERF.D7-OE#11* lines displayed a 40%–45% enhancement in lycopene levels at the Br + 10 stage compared with WT fruits, consequently imparting them an intense red color phenotype (Figure 4A). Concomitantly, a sharp increase in β-carotene content was detected in *SlERF.D7* RNAi fruits at the Br + 10 stage, keeping with an orange fruit phenotype (Figure 4B). Similar to an opposite trend observed for lycopene content in OE and RNAi lines, β-carotene content also exhibited contrasting profiles in the fruits of the two sets of transgenic plants. To uncover the molecular basis of this modulation in carotenoid composition, we analyzed the transcript level of genes involved in the carotenoid biosynthetic pathway of pericarp tissue at different stages during fruit ripening by RT-qPCR. Transcript abundance of *phytoene synthase*, *PSY1*, a key regulator of the carotenoid pathway, was severely repressed in *SlERF.D7-RNAi#1* and *SlERF.D7-RNAi#4* fruits at B + 3 and later ripening stages, concomitant to the silencing pattern of this gene in the RNAi lines (Figure 4C). A similar reduction in mRNA levels of *phytoene desaturase* (*SlPDS*) was also observed in *SlERF.D7* RNAi fruits (Figure 4C). In contrast, transcripts accumulation of all the three lycopene-β-cyclases (β-*LYC1*, β-*LYC2*, and *CYC-β*) were significantly upregulated in *SlERF.D7*

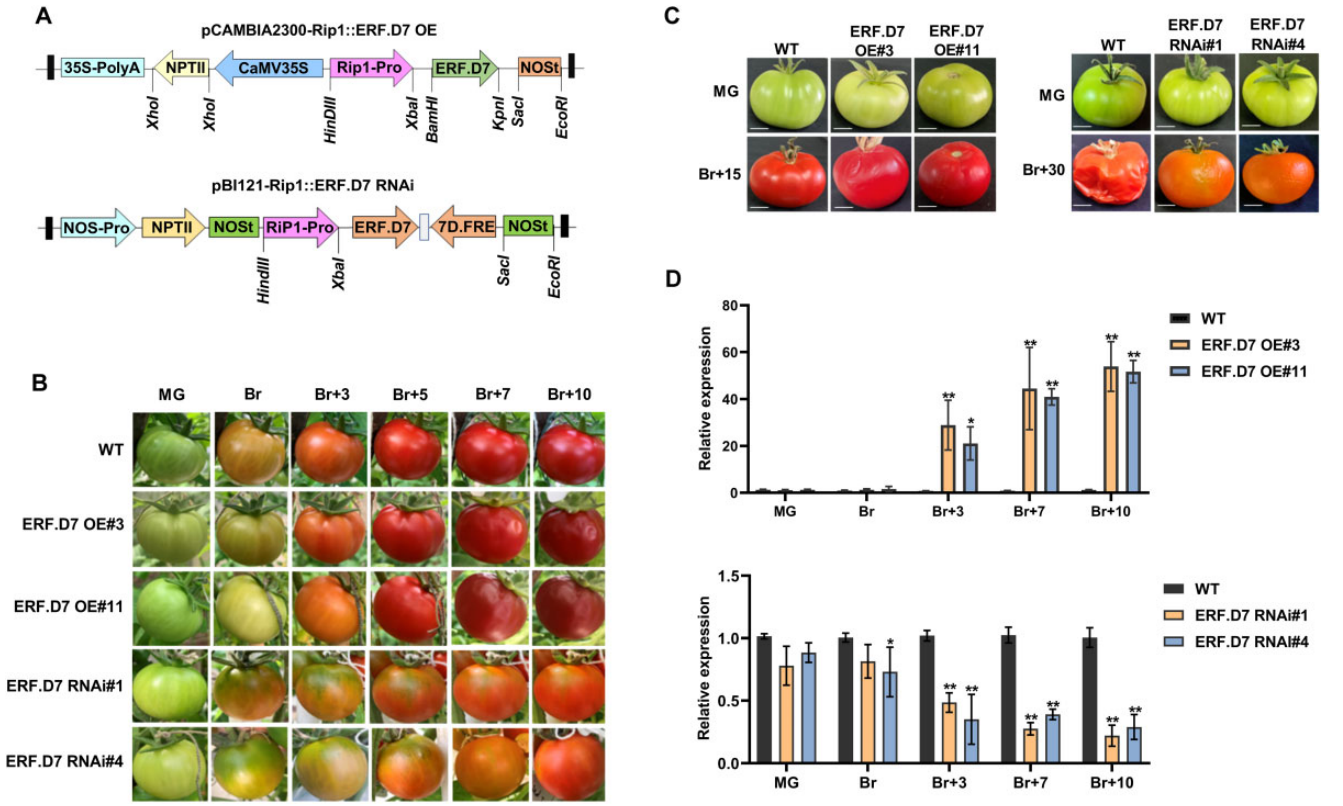

Figure 3 Morphological and molecular characterization of *SlERF.D7* OE and RNAi lines. A, Vector diagram of *pCAMBIA2300-Rip1::SlERF.D7* OE (over-expression) and *pBI121-Rip1::SlERF.D7* RNAi (silencing) construct. B, Phenotypic analysis of WT, *SlERF.D7* OE, and RNAi line fruits at MG, Br, 3-day after Br (Br + 3), 5-day after Br (Br + 5), and 7-day after Br (Br + 7). C, Off-vine phenotypic assessment of WT, *SlERF.D7* OE, and RNAi line fruits harvested at the MG stage and photographed till the first sign of shriveling appears, 15-day post Br (Br + 15) in *SlERF.D7* OE lines, and 30-day post Br (Br + 30) in *SlERF.D7* RNAi line. D, Transcript levels of *SlERF.D7* in WT, OE, and RNAi transgenic fruit analyzed at MG, Br, 3-day after Br (Br + 3), 7-day after Br (Br + 7), and 10-day after Br (Br + 10) by RT-qPCR with *Actin* gene as an internal control. Error bars mean±SD of three biological replicates. Asterisks indicate the statistical significance using Student's *t* test: *, 0.01 < *P*-value < 0.05; **, 0.001 < *P*-value < 0.01.

RNAi fruits when compared with their WT counterparts, probably responsible for the elevated β-carotene accumulation in these transgenic fruits (Figure 4C). Likewise, a substantial increase in the transcript levels of *SlPSY1* and *SlPDS* with a coordinated decline in expression levels of β-*LYC1*, β-*LYC2*, and *CYC*-β in *SlERF.D7-OE#3* and *SlERF.D7-OE#11* fruits, at Br + 3 and later stages, accounted for the enhanced carotenoid accumulation in these fruits (Figure 4C). The data indicate that repression of *SlERF.D7* culminates in modified lycopene to β-carotene ratio via the alteration in expression levels of key carotenoid pathway genes such as *PSY1*, *PDS*, and lycopene β-cyclases.

Given that fruit softening is another critical parameter of fruit ripening, we assessed the progression of firmness in *SlERF.D7* OE and RNAi lines fruits from MG to Br + 10 stage. Acceleration of 35% in fruit softening was detected in *SlERF.D7-OE#3* and *SlERF.D7-OE#11* fruits at the Br + 3 stage compared with their WT control (Figure 5A). On the other hand, *SlERF.D7* RNAi-silenced fruits were associated with a noticeable increase in fruit firmness, which reached a maximum of two to three times higher than that in WT fruit at the Br + 7 stage (Figure 5A). To further substantiate these findings at the genetic level, we examined the mRNA abundance of cell wall modifying enzymes such as polygalacturonase-2a (*PG2A*) and pectate lyase (*PL*) using RT-qPCR. *SlERF.D7-OE#3* and *SlERF.D7-OE#11* lines fruits accumulated higher *PG2A* and *PL* transcripts than the WT fruits at the Br + 3 and Br + 7 stages, consistent with the shriveled appearance of these fruits (Figure 5B). Contrastingly, transcripts levels of these two genes were significantly inhibited at the B + 3 stage onward in the fruits of *SlERF.D7* RNAi lines compared with their WT controls. Altogether, data indicate that once the ripening program initiates, it proceeds at a much more intense rate in *SlERF.D7* OE transgenic fruits and milder in the *SlERF.D7* RNAi fruits in comparison to their WT control counterparts.

Ethylene emission and perception are altered in *SlERF.D7* OE fruits

Since increased ethylene output is instrumental in determining the speed of ripening, carotenoid accumulation, and fruit firmness, we next assessed ethylene production in *SlERF.D7* OE and RNAi fruits from MG to B + 10 stage. A 40%–45% rise in ethylene emission was recorded in *SlERF.D7-OE#3* and *SlERF.D7-OE#11* transgenic fruits compared with the same-stage WT control fruits. In contrast, substantially lower

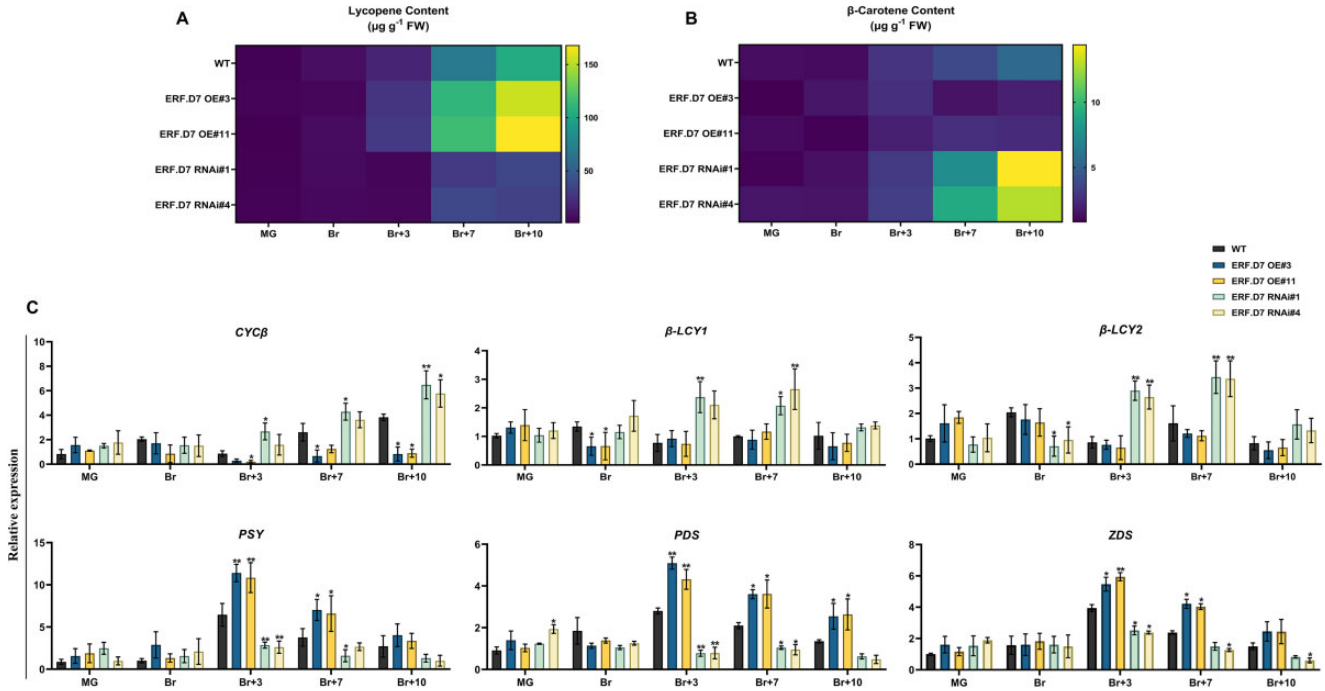

Figure 4 Pigment accumulation assessment in *SlERF.D7* OE and RNAi fruits. A and B, Estimation of (A) lycopene and (B) β-carotene in WT and *SlERF.D7* OE and RNAi lines at different stages of fruit ripening. C, RT-qPCR analysis of carotenoid biosynthetic pathway genes in WT and *SlERF.D7* OE and RNAi tomato lines at MG, Br, 3-day after Br (Br + 3), 7-day after Br (Br + 7), and 10-day after Br (Br + 10) with *Actin* gene as an internal control. Error bars are means ±SD of three biological replicates. Asterisks indicate the statistical significance using Student's *t* test: *, 0.01 < *P*-value < 0.05; **, 0.001 < *P*-value < 0.01. β-LCY1, β-LCY2, CYC-β lycopene b-cyclases; PSY1 phytoene synthase; PDS phytoene desaturase; and ZDS, carotenoid desaturase.

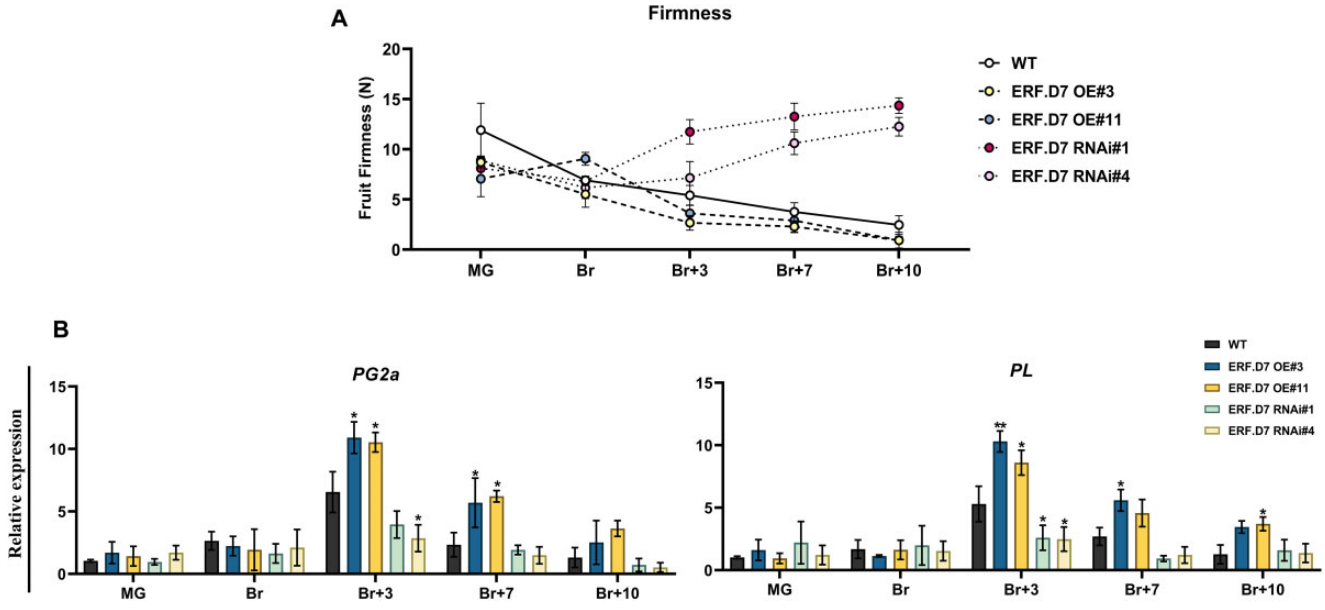

Figure 5 Modulations in levels of fruit firmness in *SlERF.D7* OE and RNAi fruits. A, Fruit firmness analysis in WT, *SlERF.D7* OE, and RNAi line fruits at different stages of ripening, with fruits being harvested at MG stage. A total of 15 fruits were used for each measurement, and the values shown are the means ±SD. B, RT-qPCR analysis of polygalacturonase gene (*SlPG2A*) and PL (*SlPL*) at MG, Br, 3-day after Br (Br + 3), 7-day after Br (Br + 7), and 10-day after Br (Br + 10) in *SlERF.D7* OE, RNAi, and WT fruits. *GAPDH* and *Actin* were used as the internal controls. The error bars represent ±SD of three biological replicates. Asterisks indicate the statistical significance using Student's *t* test: *, 0.01 < *P*-value < 0.05; **, 0.001 < *P*-value < 0.01.

ethylene production was observed in *SlERF.D7* RNAi-silenced fruits at the B + 3 stage. The atypical ethylene maxima observed at the Br + 3 stage in the WT fruits were missing in the RNAi lines fruits (Figure 6A). Assessment of the expression of key ethylene biosynthetic genes by RT-qPCR revealed elevated *SlACO1*, *SlACS2*, and *SlACS4* transcripts in *SlERF.D7* OE fruits at B + 3 or later ripening stages (Figure 6C). On the other hand, *SlERF.D7* RNAi fruits displayed reduced mRNA levels at Br + 3, Br + 7, and Br + 10 stages compared with their same-stage WT counterparts (Figure 6C). Interestingly, to compensate for low ethylene production, exogenous ethylene application to SlERF.D7 RNAi fruits at the MG stage failed to reverse the inhibited ripening phenotype (Figure 6B and Supplemental Figure S3). To corroborate this, we conducted an expression profiling of genes involved in the ethylene signaling pathway in WT, *SlERF.D7* RNAi, and OE fruits at different stages of ripening. We noticed a drastic reduction in the transcripts accumulation of ethylene receptors such as *ETR2*, *ETR3* (*NR*), *ETR4*, and *ETR5* in post Br stages of *SlERF.D7* RNAi fruits when compared with the WT fruits (Figure 6C). Among the other important ethylene signaling genes, *ethylene-insensitive 2* (*EIN2*) and *EIN2-like* (*EIL2*) were also down-regulated during ripening in *SlERF.D7* RNAi line fruits (Figure 6C). To further narrow down to ERFs, altered but mostly opposite expression patterns of numerous ERFs were observed in *SlERF.D7* OE and RNAi fruits to each other. Five ERF genes (*ERF.A3*, *ERF.C1*, *ERF.E1*, *ERF.E2*, and *ERF.E4*) displayed up-regulation at the onset of ripening starting from the Br stage in *SlERF.D7* OE lines (Supplemental Figure S4). In contrast, a concomitant decrease in transcripts of these five ERFs was observed in *SlERF.D7* RNAi fruits at post-Br stages. By contrast, the mRNA abundance of three ERFs (*SlERF.B1*, *SlERF.B2*, and *SlERF.B3*) exhibited enhanced mRNA abundance in *SlERF.D7* RNAi line fruits (Supplemental Figure S4). To rule out any possibility of off-target effects in *SlERF.D7* transgenic line, we further investigated the expression profiles of all SlERF.D clade members. We found no significant changes in any SlERF.D clade member's transcript abundance in transgenic fruits when investigated using Student's *t* test with *P*-value ranging from $0.05 < P\text{-value} < 0.001$ (Supplemental Figure S5). In conclusion, these results signify that ethylene biosynthesis coupled with ethylene perception and signaling contributes to the altered ripening phenotypes observed in the OE and RNAi lines.

Transcription of key ripening regulators is modulated in *SlERF.D7* transgenic line fruits

To unveil the possible molecular mechanism responsible for this altered ripening phenotypes of *SlERF.D7* transgenic lines, we assessed the transcript profiles of major ripening regulator genes at different stages of ripening. Compared with WT fruits, *RIN* and *CNR* mRNA levels were significantly reduced at Br + 7 and Br + 10 stages in the RNAi fruits (Figure 7). Likewise, 50%–60% reduction in the transcripts of *FRUITFUL1* (*FUL1*) and *FRUITFUL2* (*FUL2*) were observed in *SlERF.D7* RNAi fruits at post Br stages (Figure 7). Similar inhibition was also observed in mRNA levels of *NOR*, *SlAP2a*, and *TAGL1* genes in the RNAi lines fruits (Figure 7). The altered expression pattern of most of these genes in *SlERF.D7*

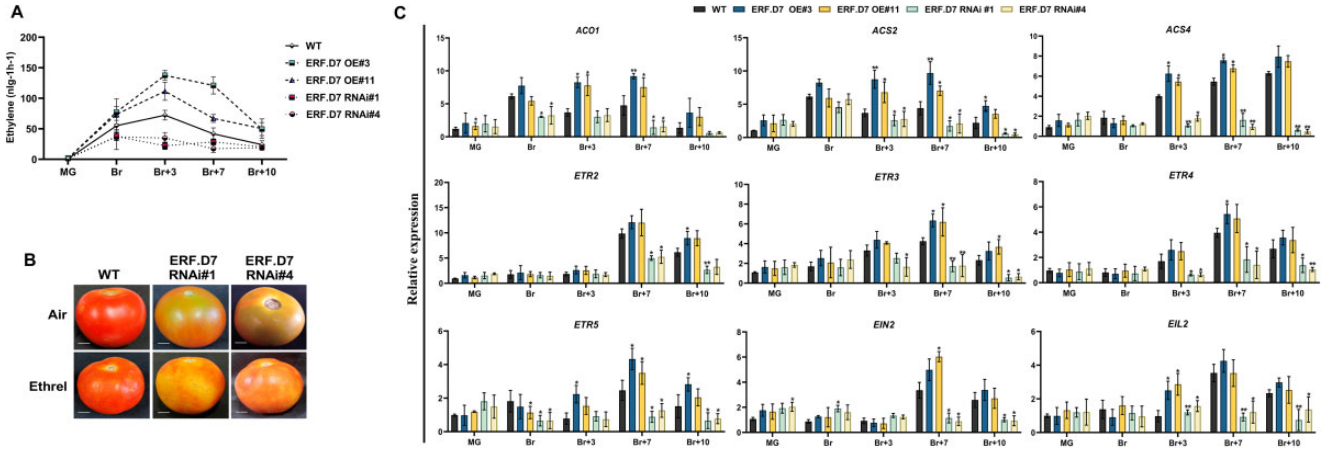

Figure 6 Alterations in ethylene biosynthesis and perception in *SlERF.D7* transgenic fruits. A, Ethylene production of WT and *SlERF.D7* OE and RNAi fruits assessed at MG, Br, 3-day after Br (Br + 3), 7-day after Br (Br + 7), and 10-day after Br (Br + 10) stages. Values represent the means of at least five individual fruits. The error bars represent ±SD of three biological replicates. B, Exogenous ethylene treatment on WT and *SlERF.D7* RNAi fruit. MG fruits from WT and *SlERF.D7* RNAi lines were injected with a buffer solution containing 10 mM MES, pH 5.6, sorbitol (3% w/v), and 100 μM ethrel (2-chloroethylphosphonic acid, 40% solution, SRL Diagnostics). After the treatment, fruits were incubated in a culture room at 26°C, under a 16-h light/8-h dark cycle with a light intensity of 100 μmol m^{-2} s^{-1} and photographed after 7 days. C, RT-qPCR analysis of ethylene biosynthesis and perception pathway genes at MG, Br, 3-day after Br (Br + 3), 7-day after Br (Br + 7), and 10-day after Br (Br + 10) in *SlERF.D7* OE, *SlERF.D7* RNAi, and WT fruits with *Actin* gene as an internal control. Error bars represent ±SD of three biological replicates. Asterisks indicate the statistical significance using Student's *t* test: *, $0.01 < P\text{-value} < 0.05$; **, $0.001 < P\text{-value} < 0.01$. ACO1, aminocyclopropane-1-carboxylic acid oxidase 1; ACS2 and ACS4, aminocyclopropane-1-carboxylic acid synthases; ETR2, ETR3, ETR4, and ETR5, ethylene receptors; EIN2, ethylene signaling protein; and EIL2, protein.

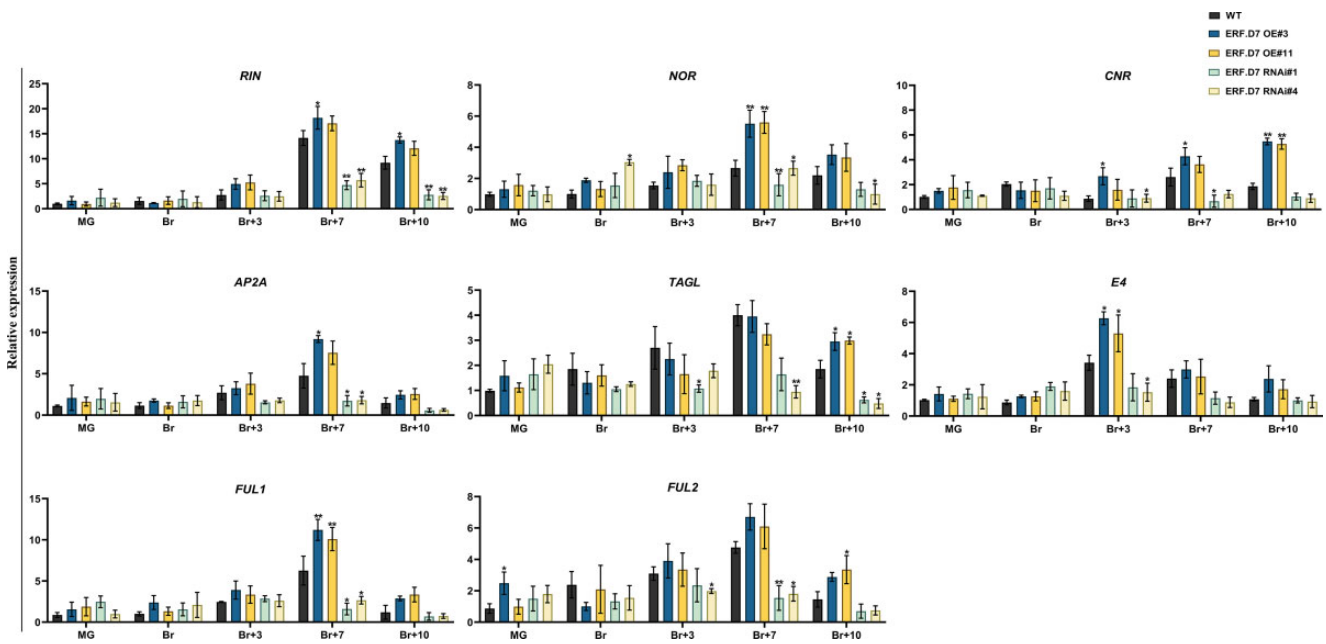

Figure 7 Transcript profiling of key ripening regulator genes in WT and *SlERF.D7* OE and RNAi tomato lines during fruit ripening. Total RNA was extracted from MG, Br, 3-day after Br (Br + 3), 7-day after Br (Br + 7), and 10-day after Br (Br + 10) stages of *SlERF.D7* OE, SlERF.D7 RNAi, and WT fruits. The relative mRNA levels of each gene were normalized using the *Actin* gene as an internal control. Error bars represent ±SD of three biological replicates. Asterisks indicate the statistical significance using Student's *t* test: *, 0.01 < *P*-value < 0.05; **, 0.001 < *P*-value < 0.01. NOR, non-ripening; CNR, colorless non-ripening; AP2a, APETALA2/ERF gene; TAGL1, tomato AGAMOUS-LIKE 1; E4, ethylene-responsive and ripening regulated genes; FUL1 and FUL2, fruitful MADS-box transcription factor homologs.

transgenic fruits is consistent with the delayed onset of ripening observed in the RNAi lines. Correspondingly, *SlERF.D7* OE fruits accumulated elevated transcripts of *RIN*, *CNR*, *NOR*, *AP2A*, and *TAGL1*, compared with the WT control fruits, at post Br stages.

SlERF.D7 alters fruit ripening by influencing auxin sensitivity

Because *SlERF.D7* positively responded to IAA treatment, and the fact that *SlERF.D7* RNAi fruits closely mimicked the ripening phenotype of *SlARF2A* and *SlARF2B* RNAi (or OE) fruits reported earlier (Hao et al., 2015; Breitel et al., 2016), we next assessed the levels of IAA in transgenic fruits at MG, Br, and Br + 7 stages. Remarkably, a significant increase in IAA concentration was observed in *SlERF.D7* RNAi fruits at the Br + 7 stage (Figure 8A). In contrast, the OE lines showed slightly decreased IAA levels. Considering the modulated IAA levels in transgenic fruits and the known roles of tomato ARFs in ripening, we then examined the expression profile of all tomato ARF gene family members by RT-qPCR (Kumar et al., 2015; Supplemental Figure S6). Strikingly, the transcript accumulation of *SlARF2* paralogs was significantly affected in the transgenic fruits. Transcription of no other ARF gene family members was affected in *SlERF.D7* transgenic fruits (Supplemental Figure S6). In particular, *SlARF2A* displayed a dramatic down-regulation in *SlERF.D7-RNAi#1* and *SlERF.D7-RNAi#4* fruits at the Br + 3 stage, whereas *SlARF2B* exhibited a slight reduction in its mRNA levels at this stage (Figure 8B). However, transcript accumulation of *SlARF2B* was reduced to 30% in *SlERF.D7* RNAi fruits at the Br + 7 stage (Figure 8A). On a similar level, *SlERF.D7* OE line fruits showed a significant upregulation in the expression of *SlARF2A* at post Br stages. These results signified a possible role of SlERF.D7 in controlling ripening traits by moderating auxin responses, plausibly through SlARF2 paralogs, in tomato fruits.

SlERF.D7 binds to and activates the promoters of *SlARF2A/B*

Because of the observed alterations in the transcript level of *SlARF2A* and *SlARF2B* in *SlERF.D7* transgenic lines fruits, we hypothesized that SlERF.D7 might bind to the promoters of the two *ARF2* paralogs. In silico analysis of 2.5-kb promoter sequences of *SlARF2A* and *SlARF2B* revealed the presence of two and three conserved ethylene responsive elements (ERE), respectively (Figure 8C). These elements are the putative targets of ERF-type transcription factors in plants. To validate this assumption, we performed a Y1H assay. A *pGAD::SlERF.D7* plasmid (containing the SlERF.D7 putative DNA domain fused to the GAL4 active domain) and a *pHIS-*cis-acting reporter construct (2-kb PCR amplified promoter regions of *SlARF2A* and *SlARF2B*) were co-transformed into yeast strain Y187. The results displayed a strong binding of SlERF.D7 to the *SlARF2A* promoter, whereas a weak interaction between this protein and *SlARF2B* promoter was noticed (Figure 8D). As indicated by the modulations in the transcript levels of these reporter genes, *SlERF.D7* could

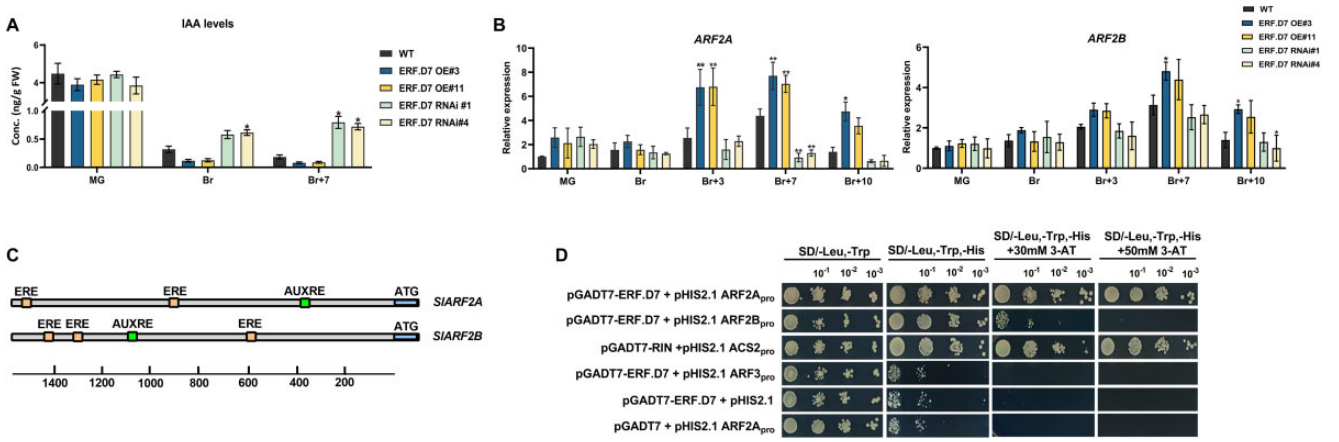

Figure 8 Altered auxin levels and ARF2 orthologs transcription in *SlERF.D7* transgenic fruits. A, Determination of IAA levels during fruit ripening in WT, *SlERF.D7* OE, and RNAi line fruits at MG, Br, and 7-day post Br (Br + 10) stages. Error bars represent ±SD of three biological replicates. Asterisks indicate the statistical significance using Student's *t* test: *, 0.01 < *P*-value < 0.05; **, 0.001 < *P*-value < 0.01. B, Expression profiling of *SlARF2* orthologs, *SlARF2A* and *SlARF2B* in transgenic fruits of *SlERF.D7* OE and RNAi lines during different fruit maturation stages, MG, Br, 3-day after Br (Br + 3), 7-day after Br (Br + 7), and 10-day after Br (Br + 10). The relative mRNA levels of both the genes were normalized using *Actin* and *GAPDH* genes as an internal control. Error bars represent ±SD of three biological replicates. Asterisks indicate the statistical significance using Student's *t* test: *, 0.01 < *P*-value < 0.05; **, 0.001 < *P*-value < 0.01. C, Analysis of putative ethylene and auxin-responsive cis-elements in the 2.5-kb promoter region of *SlARF2A* and *SlARF2B* genes. D, Y1H analysis of binding of SlERF.D7 protein to putative ethylene-responsive elements in the promoter regions of *SlARF2A* and *SlARF2B* genes displaying growth performance of transformants on SD/−Leu−/Trp/−His medium containing 50 mM 3-AT. Binding of RIN to the promoter of *SlACS2* gene-: positive control, binding of *SlERF.D7* to the promoter of *SlARF3* gene-: negative control.

directly bind to the promoters of *SlARF2A* and *SlARF2B* and regulate the expression of these target genes.

To further determine SlERF.D7-mediated direct activation of *SlARF2* genes in planta, we evaluated GUS and GFP activity driven by *SlARF2A* and *SlARF2B* promoter fusion reporter constructs in *N. benthamiana* leaves that also transiently expressed the *SlERF.D7* gene under the control of *CaMV35S* promoter (effector construct) (Figure 9, A and B). Transactivation of the *SlARF2A* promoter by SlERF.D7 significantly enhanced the GUS reporter activity. However, the transient co-expression of *SlARF2B* promoter and SlERF.D7 displayed less GUS activity elevation than *SlARF2A* and the positive controls (Figure 9C). Similar observations were made with GFP fluorescence driven by transient co-expression of *SlARF2A* and *SlARF2B* reporter constructs and SlERF.D7 effector construct in *N. benthamiana* leaves (Figure 9, B and D). Upon quantification of the relative fluorescence using flow cytometry, transactivation of *SlARF2A* reporter construct by SlERF.D7 exhibited an approximate seven-fold increase in fluorescence when compared with an approximate four-fold elevation observed in transactivation of *SlARF2B* reporter construct (Figure 9E).

The data indicate that SlERF.D7 regulates the expression of *SlARF2* paralogs by directly binding, most likely to the typical ERE elements, in their promoter regions.

Although the transient GUS and GFP transactivation assays suggested a direct regulation of *SlARF2* promoters by SlERF.D7 protein, we further conducted an electrophoretic mobility shift assay (EMSA) to assess the ability of SlERF.D7 to directly bind to *SlARF2A* and *SlARF2B* promoters. Indeed SlERF.D7 exhibited direct binding to the DNA probe containing the ERE element present in the SlARF2A promoter, whereas the unlabeled promoter fragment displaced the binding of the labeled probe in a dose-dependent manner (Figure 10A). However, SlERF.D7 displayed weak binding to ERE motif in the SlARF2B promoter (Figure 10A). These results revealed the ability of SlERF.D7 to specifically bind to ERE motif in the *SlARF2A* promoter. Combined together, the data confirm that *SlARF2* promoters are direct targets of SlERF.D7 in planta.

Silencing of *SlARF2* paralogs in *SlERF.D7* OE lines fruits partially reverse the fastened ripening phenotype

To confirm whether the elevated transcript levels of *SlARF2* paralogs were responsible for the enhanced carotenoid synthesis in *SlERF.D7* OE line fruits, we performed virus-induced gene silencing (VIGS) assays of *SlARF2A*, *SlARF2B*, and double knock-down of both *SlARF2A/B* in *SlERF.D7*-OE#3 fruits at the MG stage. A spotted ripening pattern was observed in *SlARF2A* single knock-down VIGS fruit, with the fruits remaining orange at the final maturation stage (Figure 10B). Similarly, *SlARF2B* single knock-down VIGS fruits exhibited more distinct variegation of yellow and orange color on the outer pericarp and never achieved the intense red color of *SlERF.D7* OE fruits (Figure 10B). The simultaneous double knock-down *SlARF2A/B* VIGS fruits displayed more severe ripening defects. These fruits showed mottled green and orange sectors, separated by distinct borders, contrasting with the uniform red color observed in *SlERF.D7* OE and *SlERF.D7*

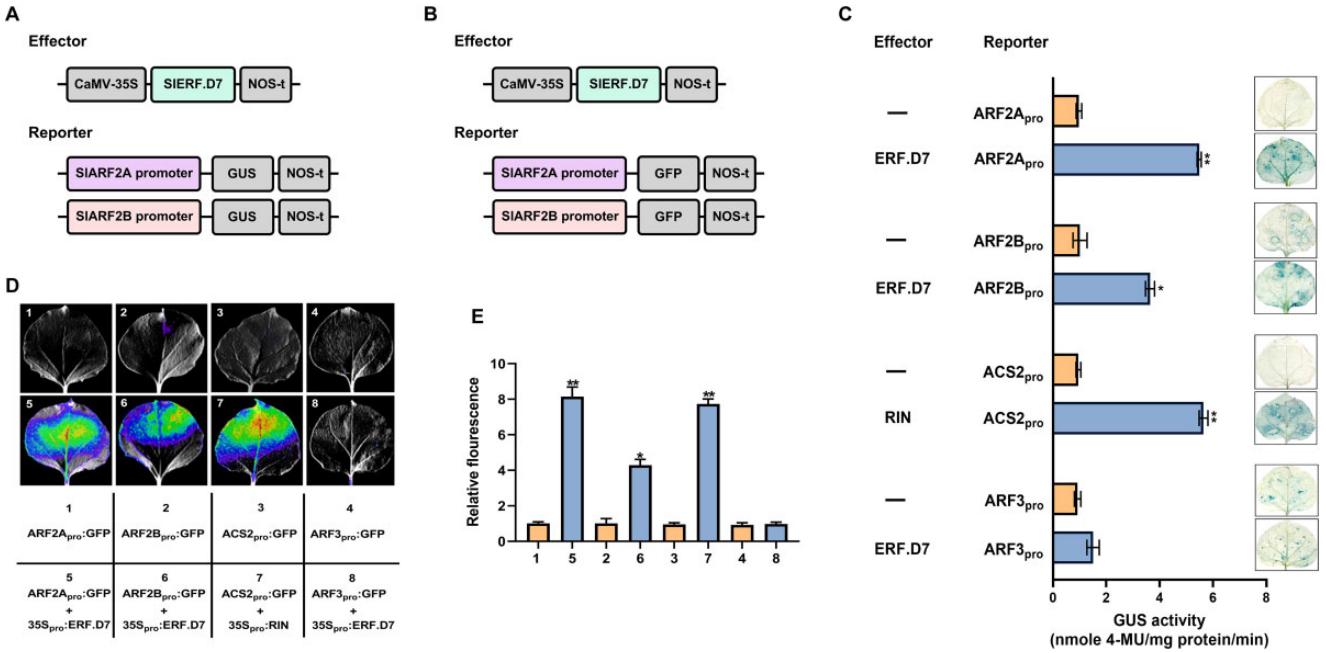

Figure 9 In vivo transactivation of SlARF2 promoters by SlERF.D7. A and B, Schematic diagrams of the reporter and effector constructs. The GUS and GFP reporter plasmids contain the promoters of *SlARF2A* and *SlARF2B*. The effector plasmids contain the *SlERF.D7* CDS under the control of the *CaMV35S* promoter. C, Confirmation of the activation of SlARF2A and SlARF2B promoters by SlERF.D7 via the GUS complementation assay in *N. benthamiana* leaves. GUS assay was performed after 48 h of infiltration. GUS activity is expressed in nmole 4-methylumelliferone mg^{-1} protein min^{-1}. Activation of the *SlACS2* promoter by RIN-: positive control, Activation of the *SlARF3* promoter by SlERF.D7-: negative control. Error bars represent ±SD of three biological replicates. Asterisks indicate the statistical significance using Student's *t* test: *, $0.01 < P\text{-value} < 0.05$; **, $0.001 < P\text{-value} < 0.01$. D and E, Transient expression assay shows that SlERF.D7 activates the expression of the GFP reporter gene. The bottom panel indicates the combination of reporter and effector plasmids infiltrated. The GFP reporter gene is driven by *ARF2A* and *ARF2B* promoters. Representative images of *N. benthamiana* leaves 48 h after infiltration captured via NightSHADE Plant Imaging System are shown. Activation of the *SlACS2* promoter by RIN-: positive control, activation of the *SlARF3* promoter by SlERF.D7-: negative control. E, Quantitative analysis of fluorescence intensity in three independent determinations was assessed. Error bars represent ±SD of three biological replicates. Asterisks indicate the statistical significance using Student's *t* test: *, $0.01 < P\text{-value} < 0.05$; **, $0.001 < P\text{-value} < 0.01$.

OE tobacco rattle virus (*TRV*) control fruits, suggesting a redundant function of *SlARF2A* and *SlARF2B* in ripening (Figure 10B). Previously, RNAi-mediated stable transgenic silencing lines of *SlARF2A*, *SlARF2B* along with a double knock-down *SlARF2A/B* have already been investigated for fruit ripening alterations by two groups (Hao et al., 2015; Breitel et al., 2016). The authors have described a similar delayed ripening phenotype in RNAi lines as we noticed with a VIGS construct in *SlERF.D7-OE#3* fruits. Also, *SlERF.D7* RNAi-silenced fruits in this study yield a similar but milder phenotype, which can be attributed to using a weaker but more ripening-specific *RIP1* promoter, instead of a constitutive *CaMV35S*, in VIGS experiments. To verify that the phenotype obtained was associated with the silencing of *ARF2A* and *ARF2B* in single and double VIGS-silenced fruits, we analyzed the expression of these genes at the molecular level. A 70%–75% reduction in transcript levels of *SlARF2* genes was observed in single and double knock-down VIGS fruits compared with *SlERF.D7-OE#3* fruits (Figure 10C). Additionally, the mRNA abundance of *SlARF2B* in *SlARF2B* single and double knock-down VIGS fruits decreased to about 15%–20% of their control OE fruits (Figure 10C).

HPLC-based assessment of color change in VIGS fruit for lycopene and β-carotene further emphasized the difference in carotenoid production in *SlERF.D7-OE#3* and its SlARF2 paralogs VIGS fruits. The lycopene levels were significantly compromised in all the VIGS fruits, with *SlARF2A/B* double knock-down fruits displaying the maximum reduction (Figure 11). In the context of β-carotene, an increase of 40%–45% was observed in *SlARF2B* lines compared with *SlERF.D7-OE#3* line control fruits (Figure 11). Therefore, it can be interpreted that this decreased lycopene and increased β-carotene levels were responsible for the yellow–orange phenotype observed in *ARF2* VIGS *SlERF.D7-OE#3* line fruits. Furthermore, *SlARF2A/B* VIGS fruits exhibited maximum fruit firmness followed by *SlARF2B* and *SlARF2A*, thereby indicating that a noticeable delay in ripening of VIGS fruits was due to reduced transcript accumulation of *SlARF2* paralogs (Figure 11). Further, *ARF2A/B* VIGS fruits displayed the lowest ripening index, followed by the *SlARF2B-* and *SlARF2A*-silenced fruits, respectively (Figure 11). These results indicate that SlERF.D7 acts upstream of SlARF2 paralogs and performs its ripening-related function by directly regulating them.

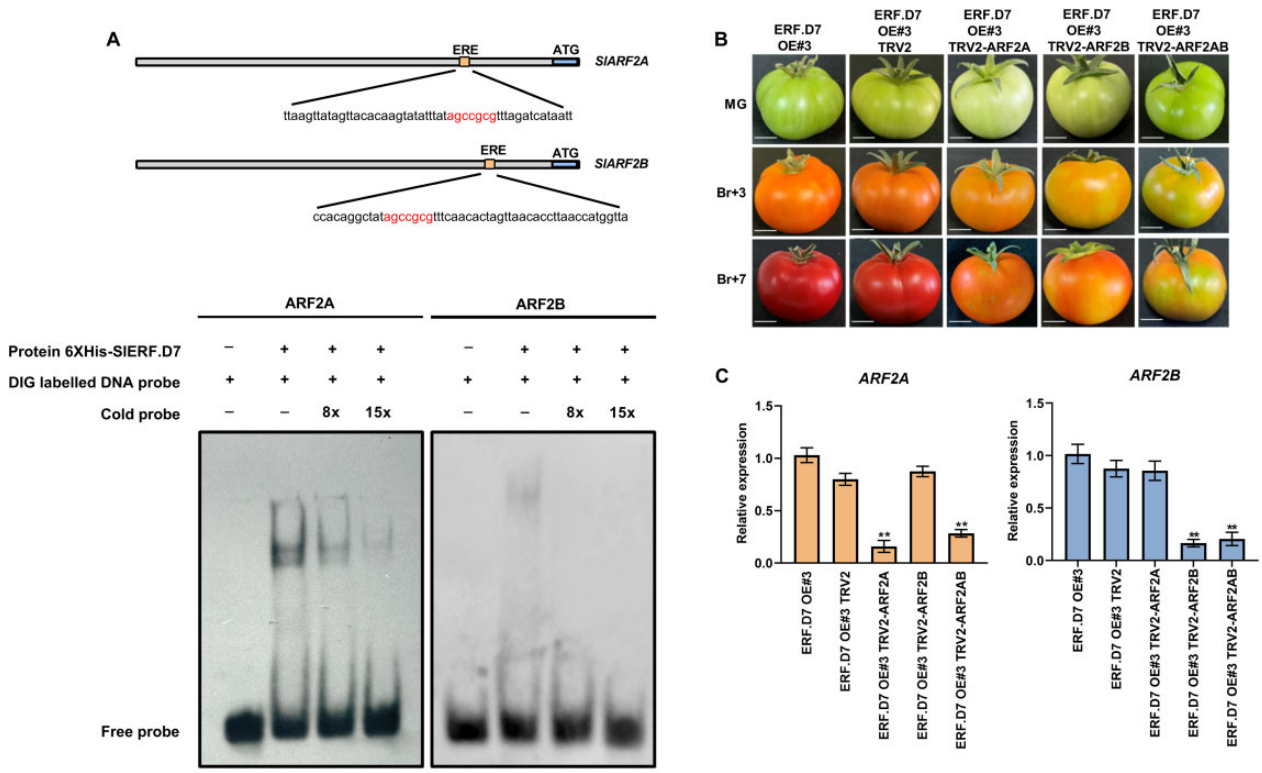

Figure 10 SlARF2 promoters are a direct target of SlERF.D7. A, SlERF.D7 binding to the promoters of *SlARF2* harboring the ERE element. The WT probe containing the ERE motif was digoxigenin-labeled. Competition for SlERF.D7 binding was performed with 8× and 15× cold probes. The symbols – and + represent the absence or presence of the probes and 6× Histidine-tagged SlERF.D7 protein. B, Phenotypes of *SlARF2A*, *SlARF2B*, and *SlARF2AB* silenced fruits in *SlERF.D7* OE background. Un-infiltrated and vector-only (pTRV) fruits were used as the control. Photographs were taken at MG, 3-day post Br (Br + 3), and 7-day post Br (Br + 7) stages. C, The silencing efficiency of the *SlARF2* orthologs in *SlARF2A*, *SlARF2B*, and *SlARF2AB* infiltrated fruits. The relative mRNA levels of both the genes were normalized using *GAPDH* and *Actin* gene as an internal control. Error bars represent ±SD of three biological replicates. Asterisks indicate the statistical significance using Student's *t* test: *, $0.01 < P\text{-value} < 0.05$; **, $0.001 < P\text{-value} < 0.01$.

Discussion

SlERF.D7, a ripening-associated gene, encodes a nuclear-localized transcriptional activator

Tomato fruit ripening is a multilayer perception process in which different hormonal inputs operate in parallel or at various levels to define an output transcriptome. For years, the center stage of this ripening process has been occupied by ethylene (Giovannoni, 2004). However, given a large number of ERFs are present in fruit species and the fact that ripening-related roles of many of these are yet to be elucidated, the complete molecular circuitry by which ethylene regulates the ripening-associated genes is not entirely understood (Solano et al., 1998; Pirrello et al., 2012; Liu et al., 2016; Srivastava and Kumar, 2019). For the last two decades, patterns of mRNA accumulation of tomato ERF gene family members during ripening have been under scrutiny. Among the 77 ERFs characterized in tomato, the expression dynamics of several ERFs have demonstrated a classic ripening-associated behavior with an increase in their transcript levels at the onset of ripening, peaking at 5 days post Br, followed by a subsequent decline at late ripening stages (Sharma et al., 2010; Liu et al., 2016). So far, a limited number of ERFs have been functionally validated for their role in regulating tomato fruit ripening (Liu et al., 2016). In this regard, the current study presents several lines of evidence substantiating the physiological importance of SlERF.D7 as an active ripening modulator which corroborates with the well-documented involvement of ERFs in tomato fruit ripening (Srivastava and Kumar, 2019). The presence of ethylene-responsive elements in the promoter region of *SlERF.D7* and its direct regulation by ethylene forms the first line of evidence on this subject. The comprehensive expression profiling of *SlERF.D7* during different stages of fruits in WT, RIN-silenced genotypes, and ripening impaired *rin* and *nor* mutants further establish a strong positive link between SlERF.D7 and tomato fruit ripening in multiple genetic backgrounds. A strong transactivation potential in yeast coupled with exclusive nuclear localization, SlERF.D7 protein displays consistency in being designated as a transcriptional factor, as shown previously for the key ripening regulator RIN protein (Ito et al., 2008). Although the mRNA abundance of *SlERF.D7* is dramatically repressed in *rin* mutant fruits in parallel with the presence of CArG box in its promoter region, the present research indicates that SlERF.D7 and RIN do not seem to operate in the same regulatory network and its ripening-associate

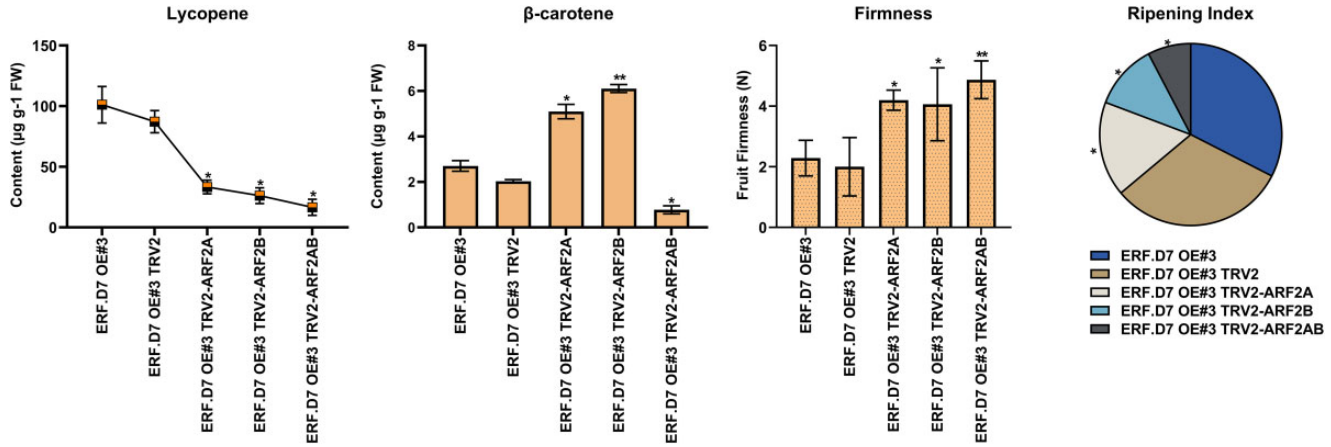

Figure 11 VIGS of *SlARF2* orthologs in *SlERF.D7* OE transgenic fruits. Assessment of lycopene, β-carotene, fruit firmness levels and ripening index in *SlERF.D7* OE, *SlERF.D7* OE TRV (control), and the *ARF2A*, *ARF2B*, and *ARF2AB* VIGS-silenced fruits. Error bars represent ±SD of three biological replicates. Asterisks indicate the statistical significance using Student's *t*-test: *, 0.01 < *P*-value < 0.05; **, 0.001 < *P*-value < 0.01.

transcription is possibly controlled by some other ripening regulator.

SlERF.D7 influences all the major facets of fruit ripening

To functionally validate the importance of SlERF.D7 in the ripening process, we generated stable OE and RNAi transgenic lines of *SlERF.D7* using a fruit ripening-specific *RIP1* promoter (Agarwal et al., 2017). *RIP1* promoter was used in this study to avoid any pleiotropic non-ripening effects in the *SlERF.D7* transgenic lines. The altered phenotypes associated with over and underexpression of *SlERF.D7*, such as ethylene production and fruit pigmentation, signify that this transcription factor broadly impacts the fruit ripening process. As per the fact that a respiratory burst coupled with an increase in ethylene production at the onset of ripening is a hallmark of the climacteric fruits, such as tomato, measurements of ethylene emission in OE and RNAi fruits were in synchronization with the observed delay in ripening of *SlERF.D7* RNAi fruits and an early ripening in the fruits of *SlERF.D7* OE lines (Alexander and Grierson, 2002; Giovannoni, 2004). The paramount role of ACC synthase and ACC oxidase genes in mediating the fruit transition from System 1 (auto-inhibitory) to System 2 (auto-catalytic) ethylene production is well known. Tomato *ACS1* and *ACS6* have shown to mediate System 1 ethylene production in immature fruit, whereas the induction of *ACS2*, *ACS4*, *ACO1*, and *ACO4* genes brings about the characteristic sharp increase in ethylene biosynthesis in System 2 (Nakatsuka et al., 1998; Barry et al., 2000; Barry and Giovannoni, 2007). The suppression of these genes has been found to inhibit tomato fruit ripening (Hamilton et al., 1990; Oeller et al., 1991; Lincoln et al., 1993; Nakatsuka et al., 1998; Barry et al., 2000). A disturbed expression pattern of *SlACO1*, *SlACS2*, and *SlACS4* genes in *SlERF.D7* transgenic fruits is seemingly responsible for the altered ethylene levels observed in these fruits. Strikingly, exogenous ethylene treatment to compensate for low ethylene levels observed in *SlERF.D7* RNAi fruits failed to restore the normal ripening process. This impairment of *SlERF.D7* RNAi fruits to activate autocatalytic ethylene production could result from the inhibited transcript levels of ethylene receptor genes, *SlETR2*, *SlETR3*, *SlETR4*, and *SlETR5*. A critical evaluation of the contribution of the *SlETR3* (*NR*) receptor in regulating ethylene biosynthesis and carotenoid accumulation has already been well-documented (Tieman et al., 2000). However, targeting a single ethylene receptor to achieve a delay in fruit ripening has been reported to result in compensatory over-expression dynamics of other ethylene receptor genes (Tieman et al., 2000). Thus, the inhibition of four ethylene receptors could account for a considerable loss of ability to perceive and channel the ethylene responses to downstream targets in the RNAi fruits. The inhibited ethylene signaling was validated by the downregulation of EIN2 and EIL3 transcripts, the positive regulators of ethylene responses, in *SlERF.D7* RNAi fruits, which may explain the defective ripening phenotype. Downstream of EILs, the signal branches to ERFs, manipulation of which can result in alterations specific to color, flavor, and texture during ripening (Liu et al., 2015, 2016; Xie et al., 2016). Notably, a report on the functional relevance of SlERF6 in mediating carotenoid accumulation during ripening has already been published (Lee et al., 2012). Another APETALA2/ERF gene family member, SlAP2a, negatively regulates tomato fruit ripening (Chung et al., 2010; Karlova et al., 2011). Also, downregulation of another ERF, SlERF.B3, via the dominant repressor technology has been shown to cause a delay in tomato ripening (Liu et al., 2014). On analyzing the expression profiles of major ERFs, *SlERF.D7* transgenic fruits displayed dramatic modulations in transcript accumulation of a high number of ERFs consistent with alterations in ethylene production and observed ripening phenotypes. A disparity in mRNA levels of *SlERF.E1* in SlERF.D7#OE and SlERF.D7#RNAi lines is interesting and needs further investigation to validate if it is upregulated due to fluctuations in the transcript abundance of *SlARF2A* and *SlARF2B* (Hao et al., 2015).

The enhanced lycopene accumulation during tomato fruit ripening is promoted by an up-regulation of *PSY1* and *PDS* and concomitant repression of lycopene cyclases transcripts. Contrastingly, inhibition in the expression of *PSY1* and *PDS* and the enhanced expression of β-*LYC* and *CYC*-β cyclases promote the conversion of lycopene to β-carotene in tomato fruits (Giuliano et al., 1993; Fray and Grierson, 1993; Pecker et al., 1996; Ronen et al., 2000; Fantini et al., 2013; Liu et al., 2014). Compared with the WT, lycopene to β-carotene ratio in transgenic fruits is substantially modified, conferring a deep red color to *SlERF.D7* OE fruits whereas imparting an orange coloration to *SlERF.D7* RNAi fruits at Br + 10 stage. This off-balance is probably a result of modulations in transcript levels of *SlPDS*, *SlPSY1*, and *SlCYCB* genes. The incapacity of *SlERF.D7* RNAi fruits to reach a red color could also be attributed to low levels of ethylene production as the rate-limiting enzyme of carotenoid biosynthesis, *SlPSY1*, is known to be ethylene inducible (Fraser et al., 1994). Apart from severe impairment of ethylene biosynthetic genes, the effect of *SlERF.D7* RNAi on the transcript levels of carotenoid pathway genes may also result from the down-regulation of the ripening master regulators, such as *RIN*, *NOR*, and *CNR*. These TFs are known to impact carotenoid accumulation in tomato fruits (Alba et al., 2005; Manning et al., 2006; Vrebalov et al., 2009; Osorio et al., 2011). In addition, the enhanced expression of *SlLCYB* and *SlCYCB* in *SlERF.D7* RNAi fruits perfectly explains the changes in carotenoid content and pigmentation observed in these fruits.

The impact of altered transcript levels of *SlERF.D7* on fruit firmness was evident from the texture analysis of *SlERF.D7* OE and RNAi transgenic lines. Numerous studies have elucidated the importance of early cell wall disintegration as one of the biggest challenges responsible for the post-harvest deterioration of tomato fruit (Meli et al., 2010; Yang et al., 2017). Although PG2a, PL, and PME enzymes are considered the major contributors to the cell wall degradation process, no significant fluctuations were observed in fruit texture in knockout fruits of *PG2a* (Grierson et al., 1993; Hall et al., 1993; Yang et al., 2017). However, CRISPR-generated mutation in *PL* resulted in firmer fruits with increased shelf life (Li et al., 2019). The enhanced softening phenotype of *SlERF.D7* OE fruits is in line with the elevated transcript levels of both *SlPG2a* and *SlPL* at late-Br stages. It is widely accepted that RIN has hundreds of target genes, including those involved in pathways regulating cell wall loosening, such as *PG2a* (Fujisawa et al., 2011, 2013; Zhong et al., 2013). We speculate that the OE of RIN in *SlERF.D7* OE fruits may also contribute to the early fruit softening phenotype observed in these fruits. Likewise, a significant reduction in mRNA accumulation of *SlPL* and *SlPG2a* combined with the decreased levels of *RIN* in *SlERF.D7* RNAi fruits impeccably synchronizes with fruit firmness studies and the phenotype associated with down-regulation of *SlERF.D7*.

SlERF.D7 regulates the expression dynamics of major ripening regulators

Tomato genetics and genomics resources are very well developed due to detailed and informative research on pleiotropic mutants such as *rin*, *nor*, and *cnr* (*colorless nonripening*) (Vrebalov et al., 2002; Giovannoni, 2004; Manning et al., 2006; Barry and Giovannoni, 2007). Inhibition of these genes dramatically and irreversibly impairs the ripening signaling cascade and therefore is termed as master regulators of fruit ripening. Interestingly, *SlERF.D7* RNAi lines fruits also display analogous through milder ripening defects as that of *rin* and *nor* mutant fruits, such as low ethylene emission, disturbed carotenoid accumulation, with altered fruit levels firmness. At the genetic level, ripening-specific silencing of *SlERF.D7* exhibits strong repression of *RIN*, *NOR*, and *CNR* genes at late-Br stages, plausibly contributing to the incompetency of the RNAi fruits to ripen normally. Apart from RIN, other MADS-domain containing transcription factors such as FUL1, FUL2, and AGAMOUS-like1 (TAGL1) play critical roles in fruit ripening regulation by forming multimeric protein complexes with RIN. Suppression of these genes substantially inhibits ripening by blocking ethylene biosynthesis and decreases carotenoid accumulation (Leseberg et al., 2008; Vrebalov et al., 2009; Itkin et al., 2009; Martel et al., 2011; Bemer et al., 2012). Previous reports on the down-regulation of *TAGL1* have shown to yield a yellow–orange pigmented fruit phenotype accompanied by a drastic decrease in levels of ethylene (Itkin et al., 2009; Vrebalov et al., 2009). In addition, *FUL1* and *FUL2* are functionally redundant in controlling the expression module of pigment-producing genes during ripening (Bemer et al., 2012). Interestingly, the fruit phenotypes observed in *FUL1*, *FUL2*, and *TAGL1* suppression lines are similar to the orange-colored *SlERF.D7* RNAi-silenced fruits. Correspondingly, the transcript abundance of these genes in *SlERF.D7* RNAi fruits displays a downward expression profile, keeping in line with the observed phenotype of these fruits. Taken together, *SlERF.D7* emerges as a critical networking component that is transcriptionally wired into a complex regulatory interplay involving several MADS-box proteins essential for ripening to occur.

SlERF.D7 integrates ethylene and auxin signal transduction pathways via the activation of *SlARF2* paralogs during ripening

Ethylene and auxin signaling components have previously been reported to be arranged and integrated into ways that can modulate the state and output of numerous plant developmental processes. However, precise signal integrators responsible for these interactions remain poorly understood despite a well-defined networking system. There is overwhelming evidence that reinforces ethylene–auxin complex interactions at the molecular level. It has been shown that mutations in auxin signaling display abnormal ethylene responses (Pickett et al., 1990). In addition, a mutual regulation, by auxin and ethylene, of genes involved in the

biosynthetic machinery of both the hormones has also been reported (Muday et al., 2012). In this regard, ERF1 has been designated as a mediator between ethylene and auxin biosynthesis via regulating ASA1 expression in Arabidopsis during root elongation (Mao et al., 2016). Likewise, auxin biosynthesis during lateral root formation is directly impacted by AtERF109 (Cai et al., 2014). Recently, SlERF.B3 has been reported to directly target SlIAA27 in mediating root length in tomato (Liu et al., 2018). Previously, we have also demonstrated the role of SlGH3-2, a ripening-induced IAA-amido synthetase, in regulating fruit ripening aspects by controlling ethylene biosynthesis and auxin homeostasis (Sravankumar et al., 2018). This study's detailed functional analysis combined with various bioinformatic approaches has rendered SlERF.D7 an active ripening regulator. To add to the complexity, we found that SlERF.D7 functions as an integrator in the interplay between ethylene and auxin through the regulation of ARF2paralogs, members of the tomato ARF family of transcriptional regulators. The transcriptional regulation of *SlARF2* by both auxin and ethylene has already been reported (Hao et al., 2015; Breitel et al., 2016). Furthermore, SlERF.D7 positively mediates ethylene and auxin sensitivity, and its silencing results in modifications in ethylene levels, alterations in pigment accumulation, and a decrease in fruit firmness, reminiscent of the phenotypes of the tomato fruits under-expressing *ARF2* paralogs (Hao et al., 2015; Breitel et al., 2016). Apart from the resemblance in the fruit phenotypes, a slight increase in accumulation of IAA levels in *SlERF.D7* RNAi fruits, in conjunction with significant alterations in the expression of *SlARF2A* and *SlARF2B* in the silenced lines, indicates these genes to be the putative target of SlERF.D7. The presence of ERE elements in the promoters of *SlARF2A* and *SlARF2B* further supported our notion. The heterologous and in planta confirmation of SlERF.D7 binding to SlARF2A and SlARF2B promoters in yeast and *N. benthamiana*, respectively, validated this hypothesis. Consistent with the idea of SlARF2 being a direct target of SlERF.D7 in Y1H and electrophoretic mobility shift experiments, subsequent transactivation assays using GUS and GFP reporter systems in *N. benthamiana* evidently demonstrated a direct association between the two classes of transcription factors. Another key piece of evidence further substantiating the activation of *ARF2* promoters by SlERF.D7 is obtained from the VIGS assay of single and chimeric knock-down of *ARF2A/B* in *SlERF.D7* OE lines. The ripening phenotypes exhibited by *SlARF2A*, *SlARF2B*, and *SlARF2A/B* VIGS fruits are in agreement with the similarity of phenotypes observed in *SlERF.D7* RNAi and *SlARF2*-silenced fruits (Hao et al., 2015; Breitel et al., 2016). Altogether, the data reveal that SlERF.D7 acts upstream of SlARF2 transcription factors and impacts fruit ripening via their transcriptional activation.

In summary, our results underpin a prototype in which the ripening-induced ERF, SlERF.D7, emerges as a critical positive regulator of fruit ripening. SlERF.D7 amalgamates auxin and ethylene signaling pathways via regulating the transcript accumulation of SlARF2 paralogs in tomato (Figure 12). Silencing of *SlERF.D7* culminates in down-regulation of *SlARF2A* and *SlARF2B* genes, negatively impacting tomato fruit ripening. The SlERF.D7-ARF2A/B association seems critical for fine-tuning ethylene and auxins aspects, such as pigment accumulation and shelf-life during fruit ripening. Nonetheless, further research is warranted to delineate the molecular mechanisms underlying SlERF.D7 controlled ripening regulation and validate if SlERF.D7 directly activates the transcription of ripening master regulators such as RIN, NOR, and CNR by binding to their promoters. Besides identifying the transcription factor responsible for its activation during ripening, SlERF.D7 physical binding to ERE elements of the promoters of ARF2 paralogs and other transcriptionally affected genes in this study also remains to be ascertained.

Materials and methods

Plant materials and growth conditions

Tomato (*S. lycopersicum* L.cv Pusa Ruby) WT, *35S:RIN-RNAi* transgenic lines in Pusa Ruby background generated in our lab (RIAI05 and RIAI06) (http://hdl.handle.net/10603/389794), Ailsa Crag WT and *rin* (accession no. LA1795, in an unknown background) and *nor* (Ailsa Craig background) fruit ripening defective mutants were grown under standard greenhouse conditions: 14-h-day/10-h-night cycle, 25°C/20°C day/night temperature, 60% relative air humidity, and 250 µmol m^{-2} s^{-1} intense luminosity. Fruit pericarp tissue samples were collected from different fruit development and ripening stages, as described earlier (Kumar et al., 2012a,b). For the measurement of time to ripen, flowers were tagged at anthesis. The number of days counted from anthesis to the appearance of the first symptoms of ripening was designated as the number of days taken to reach the Br stage. The MG stage was fixed one day before the Br stage. All fruit stages were harvested in three biological replicates (each replicate was represented by a pool of several fruits from different plants for each genotype used in the present study). Upon harvest, fruits were snap-frozen in liquid nitrogen to avoid injury.

Plasmid construction and VIGS assay

Tobacco rattle virus (TRV)-based *pTRV1* and *pTRV2* vectors were used for VIGS experiments (Liu et al., 2002). A 300-bp fragment of the coding region corresponding to *SlARF2A* and *SlARF2B* was retrieved by us using the VIGS tool of the SOL Genomics Network Database (https://vigs.solgenomics.net/). Each 300-bp fragment was then PCR amplified from *S. lycopersicum* cv Pusa Ruby cDNA and inserted in the *pTRV2* vector using *Xba1* and *EcoR1* restriction sites for *SlARF2A* and *Xho1* and *Sac1* for *SlARF2B*. For double knock-down of *SlARF2A* and *SlARF2B*, a chimeric construct with fragments corresponding to both the genes was cloned and ligated into the same *pTRV2* vector. The primers used for VIGS assay cloning are listed in the Supplemental Table S1. The empty *pTRV* vector was used as a control in the VIGS

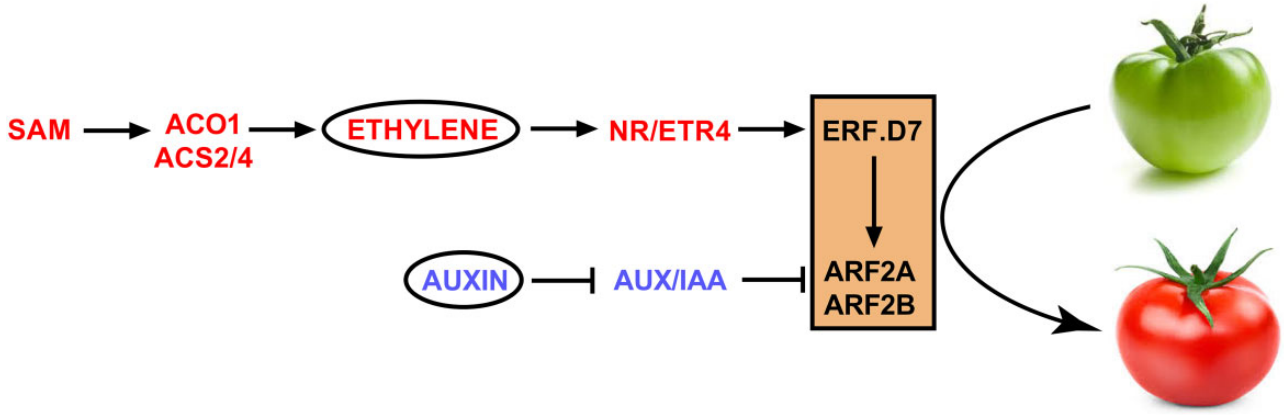

Figure 12 A general regulatory model depicting the role of SlERF.D7 in controlling tomato fruit ripening. SlERF.D7 functions in ethylene and auxin-dependent manner and directly activates the transcription of *SlARF2A* and *SlARF2B*. Thus, down-regulation of *SlERF.D7* leads to severe impairment of ARF2 orthologs and causes a delayed fruit ripening phenotype. On the contrary, OE of *SlERF.D7* promotes ripening traits by directly activating *ARF2* orthologs. Further functional and physiological dissection reveals a positive connection between the mode of action of ARF2 orthologs and fruit ripening process. Taken together, SlERF.D7 emerges as an integrator of ethylene and auxin biosynthesis and signaling pathways, which work synergistically with *SlARF2A* or with both *SlARF2A* and *SlARF2B* to achieve the competency of the fruits to ripen. SAM, *S*-adenosyl methionine; NR, never-ripe; ETR4, ethylene receptor4; and AUX/IAA, auxin/indole-3-acetic acid.

assays. The *pTRV::ARF2A*, *pTRV::ARF2B*, and *pTRV::ARF2AB* plasmids were verified by sequencing and mobilized into *Agrobacterium tumefaciens* strain GV3101. As described previously, VIGS was carried out on MG fruits (35DPA) (Fu et al., 2005).

Subcellular localization of SlERF.D7

The CDS of *SlERF.D7* was cloned in frame with GFP-reported gene into *pSITE-2CA* vector (primers are listed in Supplemental Table S1). The empty *pSITE-2CA* vector was used as a control. *SlERF.D7-pSITE-2CA* and the control vectors were transferred to *A. tumefaciens* strain GV3101 and injected into 4-week-old *N. benthamiana* leaves as described previously (Martin et al., 2009). GFP fluorescence was observed and captured by a laser confocal microscope (Leica TCS SP8, Germany) after 48 h of infiltration, as described previously by us (Kumar et al., 2015).

In silico analysis of *SlERF.D7*, *SlARF2A*, and *SlARF2B* promoters

To identify putative cis-acting elements in the promoter sequences of *SlERF.D7*, *SlARF2A*, and *SlARF2B*, 2.5-kb upstream regions from the transcription start site of each gene were retrieved from the SOL Genomics Network database. After that, the sequences were scanned using the PLACE/signal search tool (http://www.dna.affrc.go.jp/PLACE/signalscan.html) to identify ethylene/auxin/fruit-specific/ripening-related cis-acting regulatory elements.

Phytohormones treatment

For ethylene treatment to fruits, tomato fruits were harvested at the MG stage of development and injected with a buffer solution containing 10 mM MES, pH 5.6, sorbitol (3% w/v), and 100 μM of Ethrel (2-chloroethylphosphonic acid, 40% solution, Sisco Research Laboratories Pvt. Ltd., India). Similarly, auxin treatment to the MG fruits was given by injecting a buffer solution with 10 mM MES, pH 5.6, and sorbitol (3% w/v) having 100 μM IAA. For inhibitors treatment, tomato fruits harvested at Br fruits were infiltrated with the abovementioned buffer containing 100 μM 1-MCP and 100 μM PCIB, respectively. Briefly, similar-sized tomato fruits were injected using a 1-mL syringe with a 0.5-mm needle and inserted 3–4 mm into the fruit tissue through the stylar apex. The infiltration solution was gently injected into the fruit until the solution ran off the stylar apex and the hydathodes at the tip of the sepals. Only completely infiltrated fruits were used in the experiments. Control fruits were treated with the corresponding buffers only. After the treatment, fruits were incubated in a culture room at 26°C, under a 16-h light/8-h dark cycle with a light intensity of 100 μmol m^{-2} s^{-1}. After 24 h, the fruit pericarp was collected and frozen at −80°C until further use.

RNA isolation and RT-qPCR

Total RNA from the different tissues/organs/stages (cotyledon, root, leaf, stem, flower, and pericarp of fruits at IMG, MG, Br, Br + 3, Br + 5, and Br + 10) of tomato plants was isolated using RNeasy Plant Mini Kit (Qiagen, Germany) by following manufacturer's instructions. A provision for on-column DNase treatment was provided in the kit. After the RNA isolation, 1-μg of total RNA for each sample was subjected to cDNA synthesis with high-capacity cDNA reverse transcription kit (Applied Biosystems, USA), according to the instructions provided in the manual. Gene-specific primers for RT-qPCR were designed using PRIMER EXPRESS version 2.0 (PE Applied Biosystems, USA) with default parameters. Further, 2× Brilliant III SYBR Green QPCR master mix (Agilent Technologies, USA) was used for a RT-qPCR reaction carried out in a Stratagene Mx3005P qPCR machine (Agilent Technologies, USA). Three independent RNA

isolations along with three technical replicates were used for mRNA quantification. The expression values of genes were normalized using *GAPDH* and *ACTIN* gene expression values. Relative expression values were calculated by employing the $2^{-\Delta\Delta CT}$ method (Livak and Schmittgen, 2001).

Construction of *SlERF.D7* OE and silencing vectors and tomato transformation

To generate the *RIP1::SlERF.D7* OE transgenic plants, we amplified the full-length CDS and first cloned in pGEM-T Easy vector (Promega, USA) and finally mobilized into a binary vector, *pCAMBIA2300-RIP1-NOSt*, where we have already cloned the *RIP1* promoter. Similarly, to generate the *RIP1::SlERF.D7* RNAi transgenic plants, a 380-bp unique CDS of *SlERF.D7* was PCR amplified and cloned first in pUC19. The same fragment in sense and antisense orientation was cloned in juxtaposition, where an intronic sequence separated the two fragments. The assembled construct was finally mobilized into another binary vector *pBI121-RIP1-NOSt*. The cloning was confirmed by PCR, restriction digestion, and Sanger's sequencing. The sequence-confirmed OE and silencing (RNAi) plasmids were mobilized from *E scherichia coli* into *A. tumefaciens* strain AGL1. After confirmation of this mobilization, the transformed *Agrobacterium* cultures were used to generate stable transgenic *RIP1::SlERF.D7* OE and RNAi lines in Pusa Ruby, as described previously (Maligeppagol et al., 2011). Primers used in constructing *RIP1::SlERF.D7* OE and RNAi constructs are listed in Supplemental Table S1. The OE and RNAi lines were grown and analyzed for their morphological, biochemical, molecular, and physiological characterization in the T_2 generation. The segregation analysis of kanamycin resistance in T_2 progeny of *SlERF.D7 OE* and *SlERF.D7* RNAi transgenic tomato plants was done to obtain homozygous lines. Final experiments were carried out using homozygous lines from T_2 or later generations.

Fruit firmness measurement

The assessment of fruit firmness was carried out using TA.XT Plus Texture Analyzer (Stable Micro Systems, UK). Fruits that had undergone VIGS at the red ripe (Br + 7) stage were subjected to a puncture test with a 2-mm needle probe, and the force and distance measurements were recorded. Fifteen fruits from each transgenic and tissue culture generated WT genotype were used in the study. Fruit firmness calculated is equivalent to the amount of force applied to penetrate the surface of the fruit. For fruit shelf-life measurement, 10 fruits from the WT and transgenic lines were harvested at the MG stage and kept in the dark at room temperature, and photographed at regular intervals during the experiment.

Ethylene measurement

Fruits at each developmental stage were harvested and placed in open 120-mL jars for 2 h to minimize the effect of wound ethylene caused by picking. Jars were then sealed and incubated at room temperature for 35 min, and 1 mL of headspace gas was injected into an Agilent 7820A gas chromatograph equipped with a flame ionization detector (Agilent, Santa Clara, California, USA). Samples were compared with reagent-grade ethylene standards of known concentration and normalized for fruit weight. Fruits at each developmental stage were harvested and placed in open 120-mL jars for 2 h to minimize the effect of wound ethylene caused by picking. Jars were then sealed and incubated at room temperature for 35 min, and 1 mL of headspace gas was injected into an Agilent 7820A gas chromatograph equipped with a flame ionization detector (Agilent). Samples were compared with reagent-grade ethylene standards of known concentration and normalized for fruit weight. Fruits at each developmental stage were harvested and placed in open 120-mL jars for 2 h to minimize the effect of wound ethylene caused by picking. Jars were then sealed and incubated at room temperature for 35 min, and 1 mL of headspace gas was injected into an Agilent 7820A gas chromatograph equipped with a flame ionization detector (Agilent). Samples were compared with reagent-grade ethylene standards of known concentration and normalized for fruit weight.

Fruits at each developmental stage were harvested and placed in open 250-mL jars for 2 h to minimize the effect of wound-induced ethylene caused by the harvesting of the fruit. Jars were then sealed and incubated at room temperature for 4 h, and 1 mL of headspace gas was injected into Shimadzu QP-2010 Plus with Thermal Desorption System TD 20 (Shimadzu, Japan). Samples were compared with reagent-grade ethylene standards of known concentration and normalized for fruit weight. Ethylene in the headspace gas was measured thrice for each sample, with at least three biological samples for each ripening stage.

Estimation of fruit pigments

Lycopene and β-carotenoid extractions for HPLC experiments were performed as described previously (Fantini et al., 2013). Briefly, 150 mg of ground lyophilized tomato fruit powder was extracted with chloroform and methanol (2:1 v/v); subsequently, 1 volume of 50 mM Tris buffer (pH 7.5, containing 1 M NaCl) was added, and followed by the incubation of samples on ice for 20 min. After centrifugation (15,000 *g* for 10 min at 4°C), the organic phase was collected and the aqueous phase was re-extracted with the same amount of chloroform. The combined organic phases were then dried by centrifugal evaporation and resuspended in 100 µL of ethyl acetate. A final volume of 20 µL was injected into a C-18 column in HPLC (Shimadzu, Japan) analysis. For each genotype, at least five independent extractions were performed.

Estimation of titrable acids

The amount of titrable acids (TA) was determined by titrating the fruit homogenates against 0.1 N NaOH solution using phenolphthalein as an indicator to the endpoint at pH 8.1 (Singh and Pal, 2008). The TAs were measured by using the following equation:

$$\text{TA (g/100g)} = \frac{\text{Volume of NaOH used for obtaining endpoint} \times 0.6458}{\text{Weight of sample}}.$$

Determination of total soluble solids

The quantification of total soluble acids (TSSs) was done by measuring the refractive index of tomato juice through a portable refractometer (Erma Handheld Refractometer, India). The refractive index of water was initially calculated with the device to serve as zero error. A drop of the sample (tomato juice) of all the test samples was placed individually on the measuring surface beneath the Viewpoint Illuminator. Through the eyepiece, the readings were recorded at the point where the contrast line crossed the scale. The results have been expressed in degrees Brix (percentage of TSS in solution at 20°C).

The ripening index for all the samples was calculated using the following formula:

$$\text{Ripening index} = \frac{\text{Total soluble solids}}{\text{Titrable acids}}.$$

Measurement of IAA in fruit pericarp tissue

Extraction and purification of IAA were carried out as previously reported with slight modifications (Edlund et al., 1995). Frozen samples were ground in liquid nitrogen, 50 mg fresh weight of the powdered sample was mixed with 1 mL of 80% methanol containing 1% acetic acid (v/v), and 2 ng of [$^{13}C_6$]-IAA was added as an internal standard (Cambridge Isotope Laboratories, Andover, Massachusetts, USA). The sample was extracted for 2 h at 4°C under continuous shaking. After centrifugation (10,000 *g*, 5 min), the supernatant was collected and concentrated in a vacuum. The sample was resuspended in 1 mL 0.01 M HCl slurried for 10 min at 4°C under continuous shaking with 15 mg AmberLite XAD-7HP (Organo, Tokyo, Japan). After removing the supernatant, the XAD-7HP was washed twice with 1% acetic acid. Samples were then extracted with CH_2Cl_2 (once with 400 µL and twice with 200 µL), and the combined CH_2Cl_2 fraction was passed through a 0.2-µm filter. After concentration in a vacuum, the sample was analyzed by GC-MS. Five independent samples were extracted and analyzed.

Y1H assay

For Y1H experiments, 1.5 kb long promoter sequences of *SlARF2A* and *SlARF2B* were amplified using tomato (*S. lycopersicum* L.cv Pusa Ruby) genomic DNA. The amplified products were cloned into the yeast expression vector *pHIS2*.1 and co-transformed with the *pGAD-T7-SlERF.D7* into yeast strain *Y187*. The binding of RIN to the promoter of *LeACS2* was taken as a positive control for this experiment. For negative control, the interaction of *SlARF3* promoter with *SlERF.D7* was used. The DNA–protein interaction was validated by transformant growth assays on SD/-Leu/-Trp/-His plates supplemented with 50 mM of 3-AT. Primers used in this section are listed in the Supplemental Table S1.

Transactivation of *SlARF2A* and *SlARF2B* promoters in *N. benthamiana*

To verify the DNA–protein interaction in planta, 1.5 kb upstream regions of *SlARF2A* and *SlARF2B* were used to drive the expression of GUS and GFP, and were designated as reporter vectors. The effector vector was constructed by cloning the full open reading frame (ORF) of *SlERF.D7* in the binary vector *pBI121* driven by *CaMV35S* promoter. As previously described, both reporter and effector constructs were co-transformed into 4-week-old N. benthamiana leaves. GUS histochemical staining assay and GFP fluorescence measurement assay using flow cytometry (FACS calibur microflow cytometer) (Becton Dickinson, Franklin Lakes, New Jersey, USA) done after 48 h of infiltrations. The excitation for GFP was carried out by argon laser and the fluorescence was detected using a bandpass filter (530/30 nm) in the FL1 channel. The NightSHADE LB 985 (Berthold Technologies, USA) in vivo plant imaging system was employed to detect fluorescent signals with 5 s exposure time. Data were analyzed by the IndiGO software. The average fluorescence signal for each sample was collected (cps, count per second). It was normalized using the *N. benthamiana* leaves transformed with a reporter vector combined with the vector used as effector but lacking the ERF or ARF CDSs. Three independent replicates were used for each analysis. Positive and negative controls were the same as reported earlier for the Y1H assay. Primers used in this experiment are listed in the Supplemental Table S1.

Electrophoretic mobility shift assay

The full-length *SlERF.D7* CDS was cloned in frame into pET-28a (to fuse in frame with 6× Histidine tag) for heterologous protein expression. The fusion protein construct was expressed in BL21 strain of *E. coli*. Recombinant SlERF.D7-6XHIS protein was purified by Ni^{2+} gravity flow chromatography according to the manufacturer's protocol (Ni-NTA Agarose, Qiagen) as described. For EMSA, the 50-bp probe covering the ERE element (AGCCGCC) derived from *SlARF2A* and *SlARF2B* promoter was labeled with digoxigenin as per the manufacturer's protocol using DIG Oligonucleotide 3′-End Labeling Kit (Roche Diagnostics). The same unlabeled DNA fragment was used as a competitor. The binding reactions were performed at room temperature in binding buffer (10 mM Tris [pH7.5], 50 mM KCl, 1 mM DTT, 2.5% glycerol, 5 mM $MgCl_2$, 0.5 mM EDTA, and 50 ng/ml poly [dI-dC]) containing 1 µg purified SlERF.D7-6XHIS fusion protein and 5 ng probes. The reaction products were analyzed on 6% (w/v) native polyacrylamide gel electrophoresis. The products then transferred from the gel to Hybond N+ Nylon membrane (Amersham Biosciences) and detected using DIG Nucleic Acid Detection Kit (Roche Diagnostics) according to manufacturer's protocol.

GUS histochemical and activity assays

Histochemical staining of GUS in *N. benthamiana* leaves was performed as described previously. Briefly, *N. benthamiana* infiltrated leaves were harvested and incubated in a substrate solution (50 mM sodium phosphate, pH 7.5, 0.5 mM

$K_3Fe(CN)_6$, 0.5 m$MK_4Fe(CN)_6$, 1 mM X-gluc [5-bromo-4-chloro-3-indolyl-b-D-glucuronide]) at 37°C overnight. Tissues were then cleared in 70% ethanol overnight. For the fluorometric GUS assay, the infiltrated *N. benthamiana* leaf discs were homogenized in 1 mL of extraction buffer (50 mM NaH_2PO_4, pH 7.0, 10 mM EDTA, 0.1% Triton X-100, 0.1% [w/v] sarcosyl [w/v], and 10 mM β-mercaptoethanol). The homogenate was centrifuged for 10 min at 12,000 *g* at 4°C, and 100 µL of the supernatant was mixed with 900 µL of assay buffer (1 mM 4-methylumbelliferyl-D-glucuronide in the extraction buffer). The reaction mixture was incubated at 37°C for 1 h and eventually stopped by adding a stop buffer (0.2 M sodium acetate). GUS activity was normalized to protein concentration in each crude extract and was calculated as pmole or nmole of 4-methylumbelliferone (4-MU) min^{-1} mg^{-1} protein. The Bradford method assessed the protein content using bovine serum albumin as a standard.

Accession numbers

Sequence data from this article can be found in the GenBank/EMBL data libraries under accession numbers: *Sl-ERF.A3* (Solyc06g063070), *SlERF.B1* (Solyc05g052040), *SlERF.B2* (Solyc02g077360), *SlERF.B3* (Solyc05g052030), *SlERF.C1* (Solyc05g051200), *SlERF.D1* (Solyc04g051360), *SlERF.D2* (Solyc12g056590), *SlERF.D3* (Solyc01g108240), *SlERF.D4* (Solyc10g050970), *SlERF.D5* (Solyc04g012050), *SlERF.D6* (Solyc04g071770), *SlERF.D7* (Solyc03g118190), *SlERF.D8* (Solyc12g042210), *SlERF.D9* (Solyc06g068830), *Sl-ERF.E1* (Solyc09g075420), *Sl-ERF.E2* (Solyc09g089930), *SlERF.E2* (Solyc06g063070), *SlERF.E4* (Solyc01g065980), *PSY1* (Solyc03g031860), *PDS* (Solyc03g123760), *ZDS* (Solyc01g097810), *βLCY1* (Solyc04g040190), *βLCY2* (Solyc10g079480), *CYCβ* (Solyc06g074240), *ACS2* (Solyc01g095080), *ACS4* (Solyc05g050010), *ACO1* (Solyc07g049530), *E4* (Solyc03g111720), *E8* (Solyc09g089580), *PG2a* (Solyc10g080210), *RIN* (Solyc05g012020), *CNR* (Solyc02g077920), *NOR* (Solyc10g006880), *TAGL1* (Solyc07g055920), *AP2a* (Solyc03g044300), *EIN2* (Solyc09g007870), *EIL2* (Solyc01g009170), *EIL3* (Solyc01g096810), *ETR2* (Solyc07g056580), *ETR3* (Solyc09g075440), *ETR4* (Solyc06g053710), *ETR5* (Solyc11g006180), *FUL1* (Solyc06g069430), *FUL2* (Solyc03g114830), *ACO2* (Solyc12g005940), *ACO3* (Solyc07g049550), *ACO4* (Solyc02g081190), SAUR (Solyc09g007970.1.1), *ARF2A* (Solyc03g118290), and *ARF2B* (Solyc12g042070).

Supplemental data

The following materials are available in the online version of this article.

Supplemental Table S1. List of primers used in this study.

Supplemental Table S2. Segregation analysis of kanamycin resistance in T_2 progeny of *SlERF.D7 OE* and *SlERF.D7* RNAi transgenic tomato plants.

Supplemental Figure S1. DAPI staining of SlERF.D7 in *N. benthamiana*.

Supplemental Figure S2. Kanamycin-based PCR screening of *SlERF.D7* OE and silencing lines.

Supplemental Figure S3. Phenotypic time-line of ethrel-treated and non-treated control fruits from MG to red ripe stage.

Supplemental Figure S4. The expression of *ERF* genes in WT and *SlERF.D7 OE* and *SlERF.D7 RNAi* plants.

Supplemental Figure S5. The expression of ERF.D clade genes in WT and *SlERF.D7 OE* and *SlERF.D7 RNAi* plants.

Supplemental Figure S6. The expression of *SlARF* in WT and *SlERF.D7 OE* and *SlERF.D7 RNAi* plants.

Acknowledgements

The authors acknowledge the Department of Science and Technology, India, for the Purse Grant. The SAP Grant of the University Grants Commission and FIST grant of DST, India, to the Department of Plant and Molecular Biology for infrastructure support are also acknowledged.

Funding

This work is financially supported by grants received from the Department of Biotechnology (DBT), Government of India. R.K. acknowledges the Department of Science and Technology, India, for the INSPIRE-Faculty (IF-LSPA-15), Department of Biotechnology, Government of India (BT/PR31630/AGIII/103/1119/2019) and MHRD-IoE ([RC1-20-018] and [F11/9/2019-U3(A)]) grants. A.K.S. acknowledges DBT grant BT/PR6983/PBD/16/1007/2012.

Conflict of interest statement. There are no conflicts of interest to be declared.

References

Agarwal P, Kumar R, Pareek A, Sharma A (2017) Fruit preferential activity of a tomato RPP1 gene promoter in transgenic tomato and Arabidopsis. Mol Genet Genomics **292**: 145–156

Alba R, Payton P, Fei Z, McQuinn R, Debbie P, Martin GB, Tanksley SD, Giovannoni JJ (2005) Transcriptome and selected metabolite analyses reveal multiple points of ethylene control during tomato fruit development. Plant Cell **17**: 2954–2965

Alexander L, Grierson D (2002) Ethylene biosynthesis and action in tomato: a model for climacteric fruit ripening. J Exp Bot **53**: 2039–2055

Barry CS, Giovannoni JJ (2007) Ethylene and fruit ripening. J Plant Growth Regul **26**: 143

Barry CS, Llop-Tous MI, Grierson D (2000) The regulation of 1-aminocyclopropane-1-carboxylic acid synthase gene expression during the transition from system-1 to system-2 ethylene synthesis in tomato. Plant Physiol **123**: 979–986

Bemer M, Karlova R, Ballester AR, Tikunov YM, Bovy AG, Wolters-Arts M, Rossetto P de B, Angenent GC, de Maagd RA (2012) The tomato FRUITFULL homologs TDR4/FUL1 and MBP7/FUL2 regulate ethylene-independent aspects of fruit ripening. Plant Cell **24**: 4437–4451

Benková E, Michniewicz M, Sauer M, Teichmann T, Seifertová D, Jürgens G, Friml J (2003) Local, efflux-dependent auxin gradients as a common module for plant organ formation. Cell **115**: 591–602

Blilou I, Xu J, Wildwater M, Willemsen V, Paponov I, Friml J, Heidstra R, Aida M, Palme K, Scheres B (2005) The PIN auxin efflux facilitator network controls growth and patterning in Arabidopsis roots. Nature **433**: 39–44

Böttcher C, Keyzers RA, Boss PK, Davies C (2010) Sequestration of auxin by the indole-3-acetic acid-amido synthetase GH3-1 in grape berry (*Vitis vinifera* L.) and the proposed role of auxin conjugation during ripening. J Exp Bot **61**: 3615–3625

Breitel DA, Chappell-Maor L, Meir S, Panizel I, Puig CP, Hao Y, Yifhar T, Yasuor H, Zouine M, Bouzayen M et al. (2016) AUXIN RESPONSE FACTOR 2 intersects hormonal signals in the regulation of tomato fruit ripening. PLoS Genet **12**: e1005903–e1005903

Cai X-T, Xu P, Zhao P-X, Liu R, Yu L-H, Xiang C-B (2014) Arabidopsis ERF109 mediates cross-talk between jasmonic acid and auxin biosynthesis during lateral root formation. Nat Commun **5**: 5833

Chung M-Y, Vrebalov J, Alba R, Lee J, McQuinn R, Chung J-D, Klein P, Giovannoni J (2010) A tomato (*Solanum lycopersicum*) APETALA2/ERF gene, SlAP2a, is a negative regulator of fruit ripening. Plant J **64**: 936–947

Edlund A, Eklof S, Sundberg B, Moritz T, Sandberg G (1995) A microscale technique for gas chromatography-mass spectrometry measurements of picogram amounts of indole-3-acetic acid in plant tissues. Plant Physiol **108**: 1043–1047

Fantini E, Falcone G, Frusciante S, Giliberto L, Giuliano G (2013) Dissection of tomato lycopene biosynthesis through virus-induced gene silencing. Plant Physiol **163**: 986–998

Fraser PD, Truesdale MR, Bird CR, Schuch W, Bramley PM (1994) Carotenoid biosynthesis during tomato fruit development (evidence for tissue-specific gene expression). Plant Physiol **105**: 405–413

Fray RG, Grierson D (1993) Identification and genetic analysis of normal and mutant phytoene synthase genes of tomato by sequencing, complementation and co-suppression. Plant Mol Biol **22**: 589–602

Fu D-Q, Zhu B-Z, Zhu H-L, Jiang W-B, Luo Y-B (2005) Virus-induced gene silencing in tomato fruit. Plant J **43**: 299–308

Fujisawa M, Nakano T, Ito Y (2011) Identification of potential target genes for the tomato fruit-ripening regulator RIN by chromatin immunoprecipitation. BMC Plant Biol **11**: 26

Fujisawa M, Nakano T, Shima Y, Ito Y (2013) A large-scale identification of direct targets of the tomato MADS box transcription factor RIPENING INHIBITOR reveals the regulation of fruit ripening. Plant Cell **25**: 371–86.

Gillaspy G, Ben-David H, Gruissem W (1993) Fruits: a developmental perspective. Plant Cell **5**: 1439–1451

Giovannoni JJ (2004) Genetic regulation of fruit development and ripening. Plant Cell **16(Suppl)**: S170–S180

Giuliano G, Bartley GE, Scolnik PA (1993) Regulation of carotenoid biosynthesis during tomato development. Plant Cell **5**: 379–387

Given NK, Venis MA, Gierson D (1988) Hormonal regulation of ripening in the strawberry, a non-climacteric fruit. Planta **174**: 402–406

Grierson D, Schuch W, Bevan MW, Harrison BD, Leaver CJ (1993) Control of ripening. Phil Trans R Soc Lond Ser B Biol Sci **342**: 241–250

Hall LN, Tucker GA, Smith CJS, Watson CF, Seymour GB, Bundick Y, Boniwell YM, Fletcher JD, Ray JA, Schuch W et al. (1993) Antisense inhibition of pectin esterase gene expression in transgenic tomatoes. Plant J **3**: 121–129

Hamilton AJ, Lycett GW, Grierson D (1990) Antisense gene that inhibits synthesis of the hormone ethylene in transgenic plants. Nature **346**: 284–287

Hao Y, Hu G, Breitel D, Liu M, Mila I, Frasse P, Fu Y, Aharoni A, Bouzayen M, Zouine M (2015) Auxin response factor SlARF2 is an essential component of the regulatory mechanism controlling fruit ripening in tomato. PLoS Genet **11**: e1005649–e1005649

Itkin M, Seybold H, Breitel D, Rogachev I, Meir S, Aharoni A (2009) TOMATO AGAMOUS-LIKE1 is a component of the fruit ripening regulatory network. Plant J **60**: 1081–1095

Ito Y, Kitagawa M, Ihashi N, Yabe K, Kimbara J, Yasuda J, Ito H, Inakuma T, Hiroi S, Kasumi T (2008) DNA-binding specificity, transcriptional activation potential, and the rin mutation effect for the tomato fruit-ripening regulator RIN. Plant J **55**: 212–223

Ivanchenko MG, Muday GK, Dubrovsky JG (2008) Ethylene–auxin interactions regulate lateral root initiation and emergence in *Arabidopsis thaliana*. Plant J **55**: 335–347

Jones B, Frasse P, Olmos E, Zegzouti H, Li ZG, Latché A, Pech JC, Bouzayen M (2002) Down-regulation of DR12, an auxin-response-factor homolog, in the tomato results in a pleiotropic phenotype including dark green and blotchy ripening fruit. Plant J **32**: 603–613

Karlova R, Rosin FM, Busscher-Lange J, Parapunova V, Do PT, Fernie AR, Fraser PD, Baxter C, Angenent GC, de Maagd RA (2011) Transcriptome and metabolite profiling show that APETALA2a is a major regulator of tomato fruit ripening. Plant Cell **23**: 923–941

Kumar R, Agarwal P, Pareek A, Tyagi AK, Sharma AK (2015) Genomic survey, gene expression, and interaction analysis suggest diverse roles of ARF and Aux/IAA proteins in Solanaceae. Plant Mol Biol Rep **33**: 1552–1572

Kumar R, Agarwal P, Tyagi AK, Sharma AK (2012a) Genome-wide investigation and expression analysis suggest diverse roles of auxin-responsive GH3 genes during development and response to different stimuli in tomato (*Solanum lycopersicum*). Mol Genet Genomics **287**: 221–235

Kumar R, Sharma MK, Kapoor S, Tyagi AK, Sharma AK (2012b) Transcriptome analysis of rin mutant fruit and in silico analysis of promoters of differentially regulated genes provides insight into LeMADS-RIN-regulated ethylene-dependent as well as ethylene-independent aspects of ripening in tomato. Mol Genet Genomics **287**: 189–203

Kumar V, Irfan M, Ghosh S, Chakraborty N, Chakraborty S, Datta A (2016) Fruit ripening mutants reveal cell metabolism and redox state during ripening. Protoplasma **253**: 581–594

Kumar R, Khurana A, Sharma AK (2014) Role of plant hormones and their interplay in development and ripening of fleshy fruits. J Exp Bot **65**: 4561–4575

Lee JM, Joung J-G, McQuinn R, Chung M-Y, Fei Z, Tieman D, Klee H, Giovannoni J (2012) Combined transcriptome, genetic diversity and metabolite profiling in tomato fruit reveals that the ethylene response factor SlERF6 plays an important role in ripening and carotenoid accumulation. Plant J **70**: 191–204

Leseberg CH, Eissler CL, Wang X, Johns MA, Duvall MR, Mao L (2008) Interaction study of MADS-domain proteins in tomato. J Exp Bot **59**: 2253–2265

Lewis DR, Negi S, Sukumar P, Muday GK (2011) Ethylene inhibits lateral root development, increases IAA transport and expression of PIN3 and PIN7 auxin efflux carriers. Development **138**: 3485–3495

Li S, Chen K, Grierson D (2019) A critical evaluation of the role of ethylene and MADS transcription factors in the network controlling fleshy fruit ripening. New Phytol **221**: 1724–1741

Li Y, Zhu B, Xu W, Zhu H, Chen A, Xie Y, Shao Y, Luo Y (2007) LeERF1 positively modulated ethylene triple response on etiolated seedling, plant development and fruit ripening and softening in tomato. Plant Cell Rep **26**: 1999–2008

Lincoln JE, Campbell AD, Oetiker J, Rottmann WH, Oeller PW, Shen NF, Theologis A (1993) LE-ACS4, a fruit ripening and wound-induced 1-aminocyclopropane-1-carboxylate synthase gene of tomato (*Lycopersicon esculentum*). Expression in *Escherichia coli*, structural characterization, expression characteristics, and phylogenetic analysis. J Biol Chem **268**: 19422–19430

Liu M, Chen Y, Chen Y, Shin J-H, Mila I, Audran C, Zouine M, Pirrello J, Bouzayen M (2018) The tomato ethylene response factor Sl-ERF.B3 integrates ethylene and auxin signaling via direct regulation of Sl-Aux/IAA27. New Phytol **219**: 631–640

Liu M, Diretto G, Pirrello J, Roustan J-P, Li Z, Giuliano G, Regad F, Bouzayen M (2014) The chimeric repressor version of an

ethylene response factor (ERF) family member, Sl-ERF.B3, shows contrasting effects on tomato fruit ripening. New Phytol **203**: 206–218

Liu M, Gomes BL, Mila I, Purgatto E, Peres LEP, Frasse P, Maza E, Zouine M, Roustan J-P, Bouzayen M et al. (2016) Comprehensive profiling of ethylene response factor expression identifies ripening-associated ERF genes and their link to key regulators of fruit ripening in tomato. Plant Physiol **170**: 1732–1744

Liu M, Pirrello J, Chervin C, Roustan J-P, Bouzayen M (2015) Ethylene control of fruit ripening: revisiting the complex network of transcriptional regulation. Plant Physiol **169**: 2380–2390

Liu Y, Schiff M, Dinesh-Kumar SP (2002) Virus-induced gene silencing in tomato. Plant J **31**: 777–786

Livak KJ, Schmittgen TD (2001) Analysis of relative gene expression data using real-time quantitative PCR and the $2^{-\Delta\Delta CT}$ method. Methods **25**: 402–408

Luschnig C, Gaxiola RA, Grisafi P, Fink GR (1998) EIR1, a root-specific protein involved in auxin transport, is required for gravitropism in *Arabidopsis thaliana*. Genes Dev **12**: 2175–2187

Maligeppagol M, Navale P, Chandra S, Asokan R, Nagesha SN (2011) An improved protocol for rapid and efficient Agrobacterium mediated transformation of tomato (*Solanum lycopersicum* L.). J Appl Horticult **13**: 3–7

Manning K, Tör M, Poole M, Hong Y, Thompson AJ, King GJ, Giovannoni JJ, Seymour GB (2006) A naturally occurring epigenetic mutation in a gene encoding an SBP-box transcription factor inhibits tomato fruit ripening. Nat Genet **38**: 948–952

Mao J-L, Miao Z-Q, Wang Z, Yu L-H, Cai X-T, Xiang C-B (2016) Arabidopsis ERF1 mediates cross-talk between ethylene and auxin biosynthesis during primary root elongation by regulating ASA1 expression. PLoS Genet **12**: e1005760

Martel C, Vrebalov J, Tafelmeyer P, Giovannoni JJ (2011) The tomato MADS-box transcription factor RIPENING INHIBITOR interacts with promoters involved in numerous ripening processes in a COLORLESS NONRIPENING-dependent manner. Plant Physiol **157**: 1568–1579

Martin K, Kopperud K, Chakrabarty R, Banerjee R, Brooks R, Goodin MM (2009) Transient expression in *Nicotiana benthamiana* fluorescent marker lines provides enhanced definition of protein localization, movement and interactions in planta. Plant J **59**: 150–162

Meli VS, Ghosh S, Prabha TN, Chakraborty N, Chakraborty S, Datta A (2010) Enhancement of fruit shelf life by suppressing N-glycan processing enzymes. Proc Natl Acad Sci USA **107**: 2413–2418

Muday GK, Rahman A, Binder BM (2012) Auxin and ethylene: collaborators or competitors? Trends Plant Sci **17**: 181–195

Nakatsuka A, Murachi S, Okunishi H, Shiomi S, Nakano R, Kubo Y, Inaba A (1998) Differential expression and internal feedback regulation of 1-aminocyclopropane-1-carboxylate synthase, 1-aminocyclopropane-1-carboxylate oxidase, and ethylene receptor genes in tomato fruit during development and ripening1. Plant Physiol **118**: 1295–1305

Negi S, Ivanchenko MG, Muday GK (2008) Ethylene regulates lateral root formation and auxin transport in *Arabidopsis thaliana*. Plant J Cell Mol Biol **55**: 175–187

Negi S, Sukumar P, Liu X, Cohen JD, Muday GK (2010) Genetic dissection of the role of ethylene in regulating auxin-dependent lateral and adventitious root formation in tomato. Plant J **61**: 3–15.

Oeller PW, Lu MW, Taylor LP, Pike DA, Theologis A (1991) Reversible inhibition of tomato fruit senescence by antisense RNA. Science **254**: 437–439

Osorio S, Alba R, Damasceno CMB, Lopez-Casado G, Lohse M, Zanor MI, Tohge T, Usadel B, Rose JK, Fei Z, **et al.** (2011) Systems biology of tomato fruit development: combined transcript, protein, and metabolite analysis of tomato transcription factor (nor, rin) and ethylene receptor (Nr) mutants reveals novel regulatory interactions. Plant Physiol **157**: 405–425.

Pecker I, Gabbay R, Cunningham FX, Hirschberg J (1996) Cloning and characterization of the cDNA for lycopene β-cyclase from tomato reveals decrease in its expression during fruit ripening. Plant Mol Biol **30**: 807–819

Pickett FB, Wilson AK, Estelle M (1990) The aux1 mutation of Arabidopsis confers both auxin and ethylene resistance 1 2. Plant Physiol **94**: 1462–1466

Pirrello J, Prasad BN, Zhang W, Chen K, Mila I, Zouine M, Latché A, Pech JC, Ohme-Takagi M, Regad F et al. (2012) Functional analysis and binding affinity of tomato ethylene response factors provide insight on the molecular bases of plant differential responses to ethylene. BMC Plant Biol **12**: 190

Rahman A, Amakawa T, Goto N, Tsurumi S (2001) Auxin is a positive regulator for ethylene-mediated response in the growth of Arabidopsis roots. Plant Cell Physiol **42**: 301–307

Ronen G, Carmel-Goren L, Zamir D, Hirschberg J (2000) An alternative pathway to beta-carotene formation in plant chromoplasts discovered by map-based cloning of beta and old-gold color mutations in tomato. Proc Natl Acad Sci USA **97**: 11102–11107

Růžička K, Ljung K, Vanneste S, Podhorská R, Beeckman T, Friml J, Benková E (2007) Ethylene regulates root growth through effects on auxin biosynthesis and transport-dependent auxin distribution. Plant Cell **19**: 2197–2212

Sagar M, Chervin C, Mila I, Hao Y, Roustan JP, Benichou M, Gibon Y, Biais B, Maury P, Latché A et al. (2013) SlARF4, an auxin response factor involved in the control of sugar metabolism during tomato fruit development. Plant Physiol **161**: 1362–1374

Schaffer RJ, Ireland HS, Ross JJ, Ling TJ, David KM (2013) SEPALLATA1/2-suppressed mature apples have low ethylene, high auxin and reduced transcription of ripening-related genes. AoB Plants **5**: pls047

Sharma MK, Kumar R, Solanke AU, Sharma R, Tyagi AK, Sharma AK (2010) Identification, phylogeny, and transcript profiling of ERF family genes during development and abiotic stress treatments in tomato. Mol Genet Genomics **284**: 455–475

Singh SP, Pal RK (2008) Controlled atmosphere storage of guava (Psidium guajava L.) fruit. Postharvest Biol Technol **47**: 296–306

Solano R, Stepanova A, Chao Q, Ecker JR (1998) Nuclear events in ethylene signaling: a transcriptional cascade mediated by ETHYLENE-INSENSITIVE3 and ETHYLENE-RESPONSE-FACTOR1. Genes Dev **12**: 3703–3714

Sravankumar T, Akash Naik N, Kumar R (2018) A ripening-induced SlGH3-2 gene regulates fruit ripening via adjusting auxin-ethylene levels in tomato (*Solanum lycopersicum* L.). Plant Mol Biol **98**: 455–469

Srivastava R, Kumar R (2019) The expanding roles of APETALA2/ethylene responsive factors and their potential applications in crop improvement. Brief Funct Genomics **18**: 240–254

Stepanova AN, Hoyt JM, Hamilton AA, Alonso JM (2005) A link between ethylene and auxin uncovered by the characterization of two root-specific ethylene-insensitive mutants in Arabidopsis. Plant Cell **17**: 2230–2242

Su L, Diretto G, Purgatto E, Danoun S, Zouine M, Li Z, Roustan J-P, Bouzayen M, Giuliano G, Chervin C (2015) Carotenoid accumulation during tomato fruit ripening is modulated by the auxin–ethylene balance. BMC Plant Biol **15**: 114

Swarup R, Parry G, Graham N, Allen T, Bennett M (2002) Auxin cross-talk: integration of signalling pathways to control plant development. Plant Mol Biol **49**: 409–424

Tieman DM, Taylor MG, Ciardi JA, Klee HJ (2000) The tomato ethylene receptors NR and LeETR4 are negative regulators of ethylene response and exhibit functional compensation within a multigene family. Proc Natl Acad Sci USA **97**: 5663–5668

Trainotti L, Tadiello A, Casadoro G (2007) The involvement of auxin in the ripening of climacteric fruits comes of age: the

hormone plays a role of its own and has an intense interplay with ethylene in ripening peaches. J Exp Bot **58**: 3299–3308

Vrebalov J, Ruezinsky D, Padmanabhan V, White R, Medrano D, Drake R, Schuch W, Giovannoni J (2002) A MADS-box gene necessary for fruit ripening at the tomato ripening-inhibitor (Rin) locus. Science **296**: 343–346

Vrebalov J, Pan IL, Arroyo AJM, McQuinn R, Chung M, Poole M, Rose J, Seymour G, Grandillo S, Giovannoni J et al. (2009) Fleshy fruit expansion and ripening are regulated by the tomato SHATTERPROOF gene TAGL1. Plant Cell **21**: 3041–3062

Xie X, Yin X, Chen K (2016) Roles of APETALA2/ethylene-response factors in regulation of fruit quality. Crit Rev Plant Sci **35**: 120–130

Yang L, Huang W, Xiong F, Xian Z, Su D, Ren M, Li Z (2017) Silencing of SlPL, which encodes a pectate lyase in tomato, confers enhanced fruit firmness, prolonged shelf-life and reduced susceptibility to grey mould. Plant Biotechnol J **15**: 1544–1555

Zaharah SS, Singh Z, Symons GM, Reid JB (2012) Role of brassinosteroids, ethylene, abscisic acid, and indole-3-acetic acid in mango fruit ripening. J Plant Growth Regul **31**: 363–372

Zhong S, Fei Z, Chen Y-R, Zheng Y, Huang M, Vrebalov J, McQuinn R, Gapper N, Liu B, Xiang J et al. (2013) Single-base resolution methylomes of tomato fruit development reveal epigenome modifications associated with ripening. Nat Biotechnol **31**: 154–159

Zouine M, Fu Y, Chateigner-Boutin A-L, Mila I, Frasse P, Wang H, Audran C, Roustan J-P, Bouzayen M (2014) Characterization of the tomato ARF gene family uncovers a multi-levels post-transcriptional regulation including alternative splicing. PLoS One **9**: e84203